Fakultät für Medizin, Klinikum rechts der Isar

Deutsches Zentrum für Neurodegenerative Erkrankungen

Abteilung für Translationale Neurodegeneration

New insights into factors affecting the pathogenesis of Progressive Supranuclear Palsy: Tau splicing and the effect of protein kinase RNA-like endoplasmic reticulum kinase (PERK) dysfunction

Daniel Mathias Julius Bruch

Vollständiger Abdruck der von der Fakultät für Medizin der Technischen Universität München zur Erlangung des akademischen Grades eines Doktors der medizinischen Wissenschaft (Dr. med. sci.) genehmigten Dissertation.

Vorsitzender: Prof. Dr. Dirk Busch

Prüfer der Dissertation:
1. Prof. Dr. Günter Höglinger
2. Prof. Dr. Stefan Lichtenthaler
3. Prof. Dr. Thomas Misgeld

Die Dissertation wurde am 03.08.2016 bei der Technischen Universität München eingereicht und durch die Fakultät für Medizin am 04.01.2017 angenommen.

Table of Contents

Abbreviations 3

Introduction....4

Progressive Supranuclear Palsy 4

Tau Protein 9

Protein kinase R (PKR)-like endoplasmic reticulum kinase (PERK) 14

PERK in Tauopathies....17

Materials and methods 19

Methods employed in “Mitochondrial Complex 1 Inhibition Increases 4-Repeat Isoform Tau by SRSF2 Upregulation” 19

Methods employed in “Early Neurodegeneration in the Brain of a Child Without Functional PKR-like Endoplasmic Reticulum Kinase” 22

Summaries of enclosed publications 26

Summary of the publication „Mitochondrial Complex 1 Inhibition Increases 4-Repeat Isoform Tau by SRSF2 Upregulation“ 26

Summary of the publication „Early Neurodegeneration in the Brain of a Child Without Functional PKR-like Endoplasmic Reticulum Kinase“ 27

Discussion....29

References....32

Acknowledgements 40

Enclosed publications 42

Abbreviations

ATP	Adenosine triphosphate
ATF4	Activating transcription factor 4
ATF6	Activating transcription factor 6 (ATF6)
BiP	Binding immunoglobulin protein
EIF2A	Eukaryotic translation initiation factor 2-alpha
EIF2AK3	Eukaryotic translation initiation factor 2-alpha kinase 3, here used as a description for the PERK gene only.
ER	Endoplasmic reticulum
IRE1	endoplasmic reticulum to nucleus signalling 1
MAPT	Microtubule associated protein tau, here used as a description of the tau gene only.
MTT	Thiazolyl Blue Tetrazolium Blue
NRF2	Nuclear factor erythroid 2-related factor 2
Pa	PERK activator CCT020312
PERK	Protein kinase R (PKR)-like endoplasmic reticulum kinase, also known as pancreatic endoplasmic reticulum kinase or eukaryotic translation initiation factor 2-alpha kinase 3
Pi	PERK inhibitor GSK2606414
PSP	Progressive Supranuclear Palsy
SEM	Standard error of the mean
Tg	Thapsigargin
UPR	Unfolded protein response
WRS	Wolcott Rallison Syndrome
ZNP	Zentrum für Neuropathologie und Prionenforschung, Ludwig-Maximilians Universität München.

Introduction

Progressive Supranuclear Palsy

Background

Progressive Supranuclear Palsy (PSP), also named Steele-Richardson-Olszewski disease, is a rare tauopathy of largely unknown aetiology with a prevalence of 5 – 6 per 100,000 (Nath et al. 2001). After Parkinson's disease this makes it the second most common form of degenerative Parkinsonism (Litvan and Hutton 1998). Tauopathies are a group of heterogeneous neurodegenerative diseases which have the feature of intracellular tau protein aggregation in common.

One of Charcot's pupils, Dutil, may have been the first to describe the disease in 1889 from a medical perspective (Warren and Burn 2007; Goetz 1996). He published two early medical photographs showing a likely PSP patient in the "Nouvelle Iconographie de la Salpêtrière". The first well documented cases, however, were presented in a meeting of the American Neurological Association in Atlantic City, USA by J. Clifford Richardson in 1963. The name "Progressive Supranuclear Palsy" was first coined in 1964 (Steele, Richardson, and Olszewski 1964) when Steele, Richardson and Olszewski together published an article describing the syndrome in detail.

Clinical Features

The mean age of onset is approximately 63 years, and patients tend to survive for an average of 9 years from the onset of first symptoms. There is also a male predominance (Rajput and Rajput 2001). According to a clinico-pathological study (Litvan, Mangone, et al. 1996) the most common symptoms at disease onset are postural instability and falls (63%), dysarthria (35%), bradykinesia (13%), as well as visual disturbances such as diplopia, blurred vision, burning eyes, and light sensitivity (13%). The most common cause of death is pneumonia (Nath et al. 2005).

The eponymous sign of PSP is supranuclear vertical ophthalmoplegia. "Supranuclear" refers to a lesion located above the ocular motor nuclei, thus sparing ocular motor nuclei, motor neurons and muscles controlling the eye movements directly. This symptom may occur only later during disease progression, or not at all. On examination, slowed vertical saccadic movements can be observed when asking the patient to look up and down (untargeted) or to look up to the examiner's finger held above the patient's head (targeted). The untargeted saccades are affected first. Abnormalities of horizontal gaze may follow further into disease progression (Warren and Burn 2007). The result is a staring facial expression with poor eye movements, as shown in Figure 1.

Other key motor symptoms include poor mobility, falls, Parkinsonism, and bulbar symptoms. Poor mobility is probably due to a combination of bradykinesia, postural instability and opthalmoplegia (Warren and Burn 2007). PSP patients often will get up from a chair very quickly and then fall back into it ("rocket sign") (Rehman 2000). They suffer from axial rigidity and falls therefore tend to be backwards and also present a common cause of death for PSP patients. In opposition to Parkinson's disease, parkinsonian features tend to be symmetrical in PSP. 95% of patients are affected during the course of their illness (Warren and Burn 2007). Bulbar symptoms develop early and lead to disturbed speech, often severe dysarthria and dysphagia.

In addition to motor symptoms, PSP patients also develop cognitive and behavioural problems. They include apathy, depression, dysexecutive dementia (Warren and Burn 2007) and sleep disorder (Aldrich et al. 1989).

There are at least four different subtypes of PSP which vary in their precise clinical presentation:

- Richardson syndrome (or phenotype), the classic form of PSP, affecting approximately half of all patients (Stamelou et al. 2010)
- PSP with predominant parkinsonism
- PSP with pure akinesia with gait freezing
- PSP with predominant frontotemporal dementia

Figure 1: Typical facial features of a PSP patient, demonstrating supranuclear opthalmoplegia. Source: (Warren and Burn 2007). Licenced for reprint under licence number 4112691066391 © BMJ Publishing Group Ltd.

Diagnostic criteria

The diagnostic gold standard for PSP is autopsy (Respondek et al. 2013). Clinical diagnosis is very difficult as it relies on clinical features only. No diagnostic test is currently available in routine practice, although there are some CSF and imaging biomarker developments underway (Santiago and Potashkin 2014). The diagnosis is made harder further due to a large differential diagnosis, associated yet distinct syndromes and the varying clinical symptoms of PSP (Williams and Lees 2009).

The National Institute of Neurological Disorders and Stroke and the Society for Progressive Supranuclear Palsy (NINDS-SPSP) have together developed a set of "possible", "probable" and "definite" criteria for the clinical diagnosis of PSP (Litvan, Agid, et al. 1996). Neuroprotection and Natural History in Parkinson's Plus Syndromes (NNIPPS) criteria were established with the intention to improve the sensitivity of the "probable" NINDS-SPSP criteria for the purpose of clinical trials. A recent study suggests that a combination of the NINDS-SPSP "possible" and "probable" criteria may yield the highest sensitivity (Respondek et al. 2013).

Pathological Features

Gross examination of the brain in PSP patients shows midbrain and, to a lesser extent, cerebral cortical atrophy (Hauw et al. 1994). The pathological diagnosis of PSP relies on the identification of neurofibrilliary tangles in a distribution characteristic for PSP. The hallmark lesion of PSP is the globose neurofibrillary tangle, consisting largely of 4-repeat tau protein, pictured in Figure 2E. Neurofibrillary tangles are intraneuronal cytosolic hyperphosphorylated aggregates of tau protein.

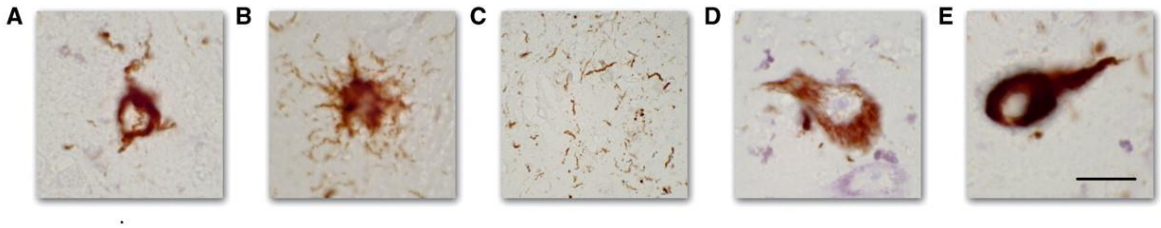

Figure 2: Neuropathological features of PSP, highlighted by the AD2 antibody. A) Cytosolic tau aggregate in oligodendrocyte. B) Tufted astrocyte. C) Neuropil threads. D) Pre-tangle. E) Globose neurofibrillary tangle. Source: (Stamelou et al. 2010). Licenced for reprint under licence number 4112691435497 ©Oxford University Press

The most consistently involved brain regions are the subthalamic nucleus, globus pallidus interna and externa, pontine nuclei, periaqueductal grey matter and the substantia nigra (Rajput and Rajput 2001).

The frontal cortex also tends to become involved at later stages of the disease (Verny et al. 1996). PSP may be distinguished from other neurofibrilliary tangle forming tauopathies through its predominant involvement of the brainstem and basal ganglia areas (Williams and Lees 2009; Hauw et al. 1994), as shown in Figure 3. However, there is significant pathological heterogeneity.

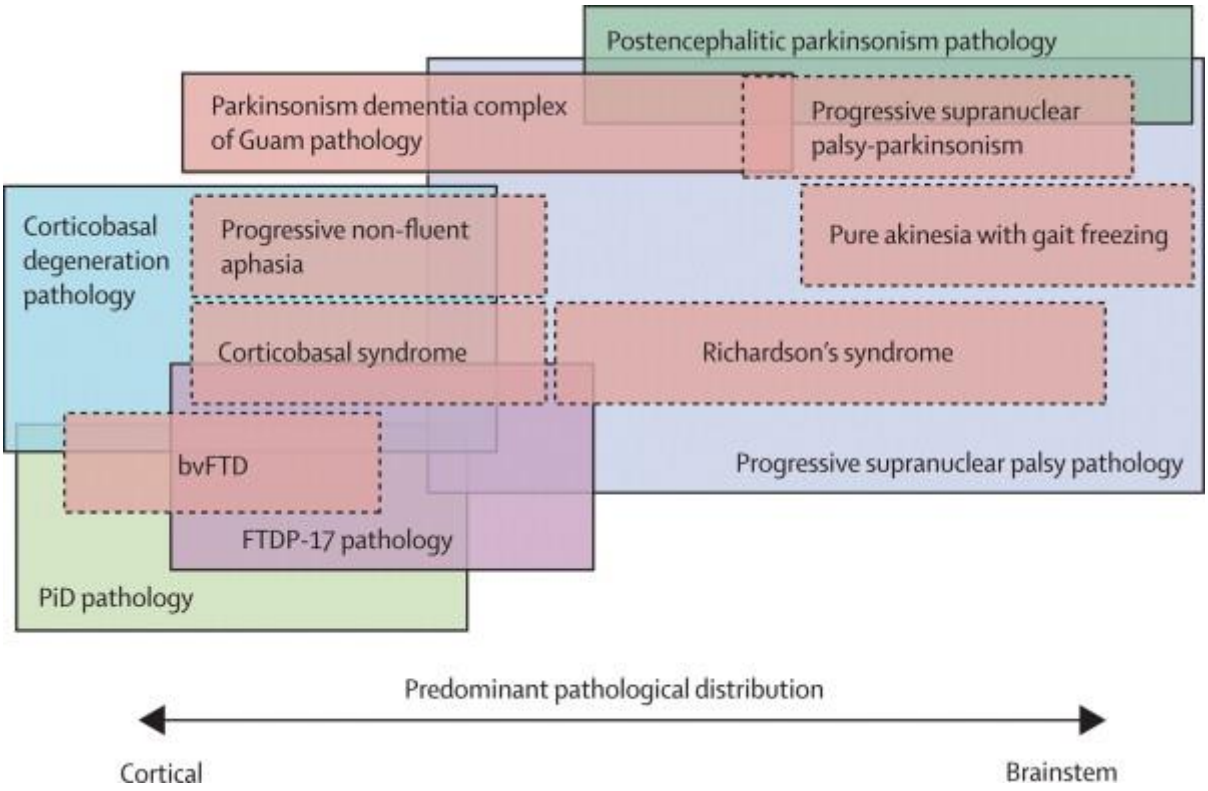

Figure 3: Predominant distribution of tau pathology in different tauopathies. Dashed boxes=clinical syndromes. Solid boxes=pathologically defined diseases. PiD=Pick's disease. FTDP-17=frontotemporal dementia with parkinsonism-17. bvFTD=behavioural variant of frontotemporal dementia. Source: (Williams and Lees 2009). Licenced for reprint under licence number 4112700248286 ©Elsevier

Aetiology

The aetiology of PSP is largely unknown. It is thought to largely occur sporadically. However, there is evidence for both genetic and environmental contributing factors.

Monogenetic causes of PSP

A PSP-like phenotype may be caused by just a single genetic mutation in the tau gene, called *Microtubule Associated Protein Tau* (*MAPT)* (Cairns, Lee, and Trojanowski 2004). Most mutations with

this effect either affect alternative splicing of exon 10, tau-tau interaction or tau-microtubule interaction.

Genetic Predisposition

In the region of the *MAPT* gene, there is a 1-Mb inversion polymorphism that contains a number of genes, including *MAPT*. This gives rise to two different haplotypes H1 and H2. The H1 haplotype is associated with PSP, with H1/H1 homozygotes making up 86.7% of PSP patients, compared to 40% of non-PSP control patients (Pastor et al. 2002). The H1 haplotype is also a risk factor for Parkinson's disease and at least three case-control studies have observed trends towards familial clustering with parkinsonism (Donker Kaat et al. 2009). However, calculations of population-attributable risk suggest that only approximately 68% of the risk of PSP can be accounted for by the *MAPT* H1 haplotype (Melquist et al. 2007).

A genome-wide association study (GWAS) was conducted in order to detect further genetic predisposing factors (Hoglinger et al. 2011). In a GWAS, single nucleotide polymorphisms (SNPs) are screened for their association with the occurrence of a disease. In the case of the GWAS for PSP, 1114 individuals with pathologically confirmed PSP (cases) and 3247 controls were screened in the first stage. Four regions featured SNPs correlated to PSP with $p < 5 \times 10^{-8}$. These were subjected to a second stage of testing with more patients (including clinically diagnosed living) in order to increase significance. The study confirmed *MAPT* as a gene highly correlated with PSP risk. However, three new genes were identified: *EIF2AK3*, *MOBP* and *STX6*.

EIF2AK3 is the gene encoding Protein Kinase R-like Endoplasmic Reticulum Kinase (PERK) and is a critical part of the unfolded protein response – the cell's natural response to an accumulation of misfolded or unfolded proteins in the endoplasmic reticulum. The correlation to PERK forms the basis of the second publication enclosed in this dissertation. *MOBP*, encoding Myelin-Associated Oligodendrocyte Basic Protein, is an abundant myelin constituent expressed by oligodendrocytes. *STX6* encodes syntaxin-6, a protein that mediates vesicle membrane fusion e.g. endosomes fusing with the membranes of the Golgi apparatus.

Environmental Risk Factors

The observation that there is an abnormally high frequency of atypical Parkinsonism on the island of Guadeloupe led to the discovery of a potential environmental cause of PSP. An epidemiological link was found between the consumption of soursop fruit (*annona muricata*) and the development of a PSP-like form of atypical Parkinsonism (Lannuzel et al. 2007). The fruit contains the acetogenin

annonacin, a potent mitochondrial complex 1 inhibitor. Annonacin was found to induce features of tauopathy *in vitro* in cultured neurons, as well as *in vivo*. In cultured neurons it causes hyperphosphorylation, redistribution of tau from the axons to the cell body and eventual cell death (Escobar-Khondiker et al. 2007; Lannuzel et al. 2003; Yamada et al. 2014). It is therefore possible that annonacin and other complex I inhibitors contribute to the pathogenesis of PSP. This environmental correlation and the features of tauopathy induced by annonacin will be the basis of the first publication enclosed in this dissertation.

Tau Protein

Physiological Function

Tau proteins were first described in 1975 by Mark Kirschner's laboratory at Princeton University (Weingarten et al. 1975). They are a group of proteins encoded by the same gene *MAPT,* but they vary by their alternative splicing pattern. Tau proteins occur most abundantly in the central nervous system but also occur elsewhere. They are found associated with microtubules and play a role in their stabilization (Weingarten et al. 1975). Further physiological functions include microtubule spacing, cellular signalling, axonal transport, neurite outgrowth and protein fibrilisation (Wade-Martins 2012). Figure 4a illustrates the way tau proteins are thought to intercalate with microtubules to stabilize them.

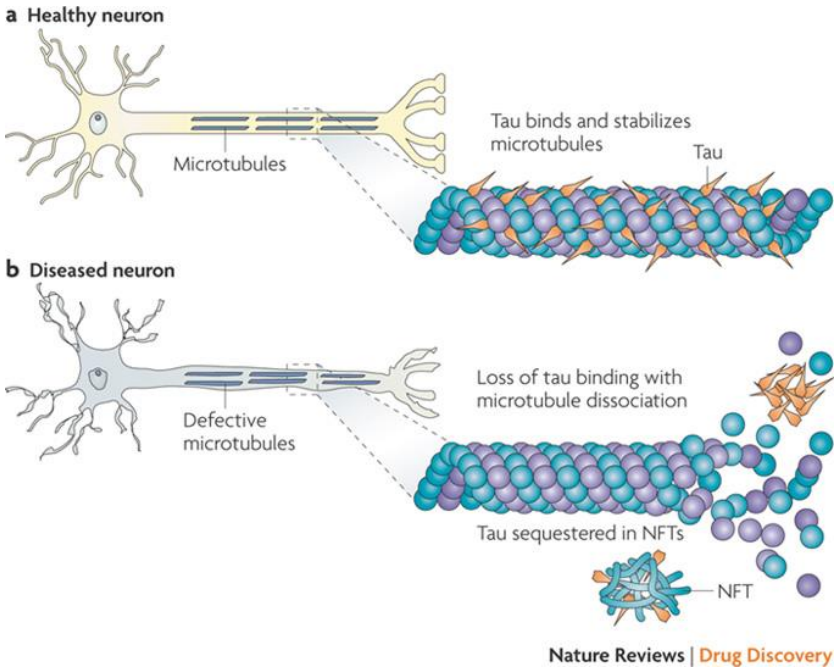

Figure 4: The structure and function of tau proteins in the physiological condition (a) and in disease (b). Source: (Brunden, Trojanowski, and Lee 2009). Licenced for reprint under licence number 4112700619210 © Nature Publishing Group

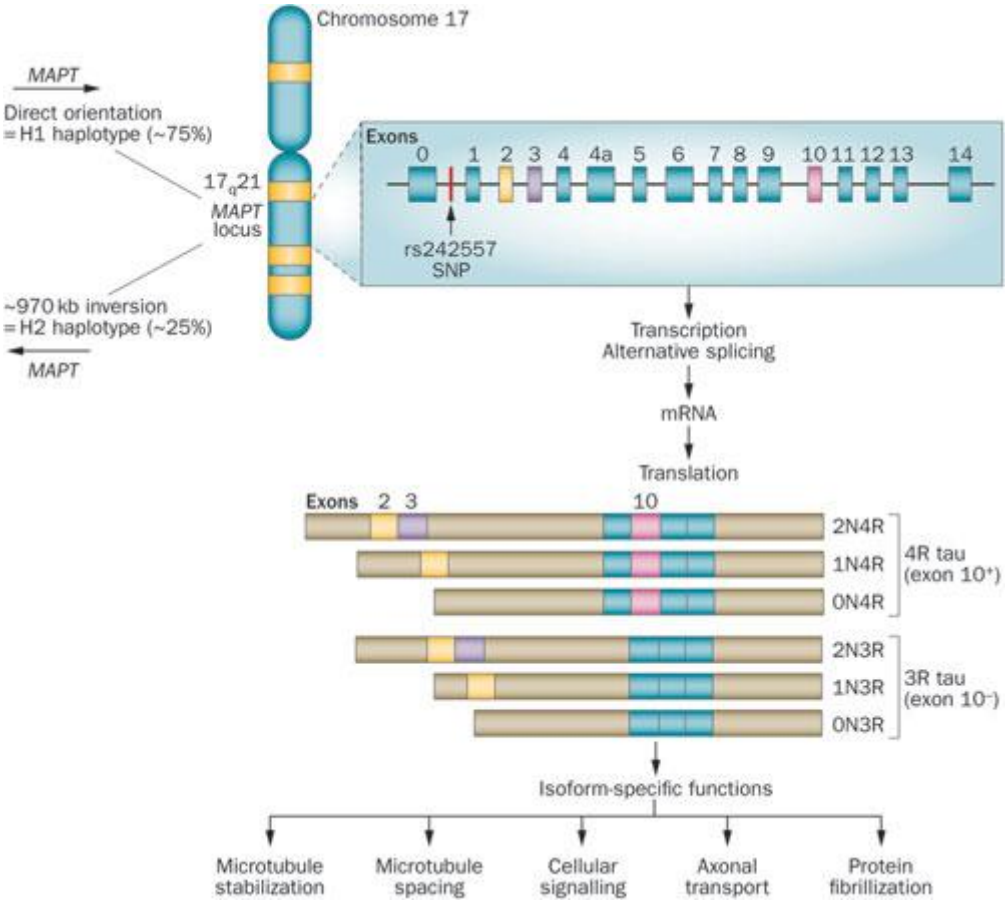

Figure 5: The alternative splicing patterns of the different MAPT isoforms. Source: (Wade-Martins 2012). Licenced for reprint under licence number 4112710002960 © Nature Publishing Group

Isoforms

As shown in Figure 5, in the human central nervous system there are six main isoforms of tau. These are distinguished by the presence of absence of exons 2, 3 and 10 by alternative splicing: 0N3R, 1N3R, 2N3R, 0N4R, 1N4R and 2N4R (Liu and Gong 2008). Exon 10 codes for a fourth microtubule binding site, therefore if it is included there are four microtubule binding sites (4R tau) and three binding sites if exon 10 is excluded (3R tau). 1N denotes the inclusion of exon 2 but not 3, whilst 2N denotes the inclusion of both exons 2 and 3.

Alternative splicing of exon 10 is under two types of control: 1) *cis*-elements in intron or exon 10 or 2) *trans*-acting factors (Liu and Gong 2008). These *trans*-acting factors are the main mechanism by which the cell actively regulates alternative splicing. *Trans*-acting factors are divided into hnRNPs (heterogeneous nuclear ribonucleoproteins) and SR (serine/arginine-rich) or SR-like proteins (Bruch et al. 2014). The SR proteins participate in the spliceosome and are involved in both constitutive splicing and regulation of alternative splicing patterns (Will and Luhrmann 2011) through control by

phosphorylation and acetylation. SR proteins are also potential drug targets and have been discussed as an option for cancer treatment (Pilch et al. 2001; Zhong et al. 2009). Their effects on tau splicing are shown in Table 1. They also play a prominent role in the first publication enclosed in this dissertation.

Table 1: Overview of the splicing factors known to influence MAPT exon 10 alternative splicing. Source: Adapted from (Liu and Gong 2008).

Splicing factor	Target *cis*-element	Effect on exon 10 splicing
SRSF1 (SRp30a, ASF)	PPE	Inclusion
SRSF2 (SRp30b, SC35)	SC35-like	Inclusion
SRSF3 (SRp20)	ND	Exclusion
SRSF4 (SRp75)	ND	Exclusion
SRSF6 (SRp55)	ND	Exclusion
SRSF7 (9G8)	ISS	Exclusion
SRSF9 (SRp30c)	ND	Inclusion
SRSF11 (SRp54)	PPE	Exclusion
TRA2B	PPE	Inclusion

Pathological Relevance

Tau proteins play a significant part in several neurodegenerative diseases, collectively known as tauopathies. Alzheimer's disease is the most common example. The mechanism of how tau proteins become pathological is largely unknown. However, substantial knowledge exists about the changes that occur to tau proteins during the pathological process. These include a conformational change, hyperphosphorylation, aggregation, prion-like spreading, as well as in some tauopathies an imbalance of the isoforms of tau.

Conformational Change

Tau proteins are so called "intrinsically disordered proteins". This means they have no stable 3D structure. A study combining simulation with small-angle X-ray scattering (Battisti, Ciasca, and Tenenbaum 2013) showed evidence of hairpin- and paperclip-like transient tertiary structures of the molecule. Monoclonal antibodies raised against tau protein extracted from Alzheimer's disease patients lead to the discovery of distinct pathological conformations of the tau protein (Jicha et al. 1997). The MC1 antibody, for example, detects a pathological conformation of tau where two parts of the tau molecule separated by more than 300 amino acids come together. It is an early marker of tau pathology (Xu et al. 2014). Two other antibodies, also raised against paired helical filament tau, Alz-50 and SMI34, likewise recognise a folded over conformation. It is therefore likely that this folding is important for the assembly of tau into paired helical filaments (Friedhoff et al. 2000).

Hyperphosphorylation

Tau protein has up to 79 potential serine and threonine phosphorylation sites, depending on the length of the isoform. In vitro, therefore, approximately 20% of the tau molecule has the potential to be phosphorylated (Goedert et al. 1989). Of these, phosphorylation has been observed in vivo on 30 different sites (Billingsley and Kincaid 1997), with different kinases and phosphatases responsible for the phosphorylation and dephosphorylation at different residues (Johnson and Stoothoff 2004).

Phosphorylation of the tau molecule seems to have several important physiological functions. Phosphorylation of certain motifs within the microtubule-binding repeats of tau strongly reduces the binding of tau to microtubules (Biernat et al. 1993). During neurite outgrowth, there is a proximal to distal gradient in tau phosphorylation at residues Ser199/202 and Thr205 along the nascent axon (Mandell and Banker 1996), suggesting a guiding role in the process. There are also changes during foetal development: foetal tau is more highly phosphorylated in the embryonic brain than adult tau (Kanemaru et al. 1992). Even anaesthesia seems to profoundly impact the phosphorylation state of tau (Run et al. 2009).

Autopsy samples from patients with virtually all tauopathies show an aberrant phosphorylation pattern (Lee, Goedert, and Trojanowski 2001). Neurofibrillary tangles in PSP and Alzheimer's disease brains stain intensely with various phospho-tau antibodies. Numerous hypotheses have been put forward regarding how the physiological process of tau phosphorylation can become pathological. A prominent theory is that phosphorylation of some residues reduces microtubule binding, thus leading to a greater pool of unbound tau and allowing free tau to aggregate (Johnson and Stoothoff 2004). Yet others believe that phosphorylation of tau may not be a pathogenic process and may rather represent a secondary event with aggregated tau being a better substrate for tau kinases[1].

Aggregation

Key intermediate steps towards the formation of neurofibrillary tangles are thought to be the formations of oligomers and paired helical filaments (PHFs) of tau. As illustrated in Figure 6, single tau proteins first form dimers either covalently by oxidation (disulphide bridge formation, stable dimer) or non-covalently (unstable dimer) (Friedhoff et al. 2000). These further oligomerise to form nuclei of several tau proteins which then further assemble by yet unknown patterns into PHFs. PHFs gained their name based on their electron-microscopic appearance of two strands twisted around one another. Although tau generally appears in the hyperphosphorylated form in PHFs, their assembly is retarded by phosphorylation (Hasegawa et al. 1997; Schneider et al. 1999).

[1] Information is based on personal communication with Prof. Dr. Michel Goedert, University of Cambridge, Cambridge, UK, Feb 2013.

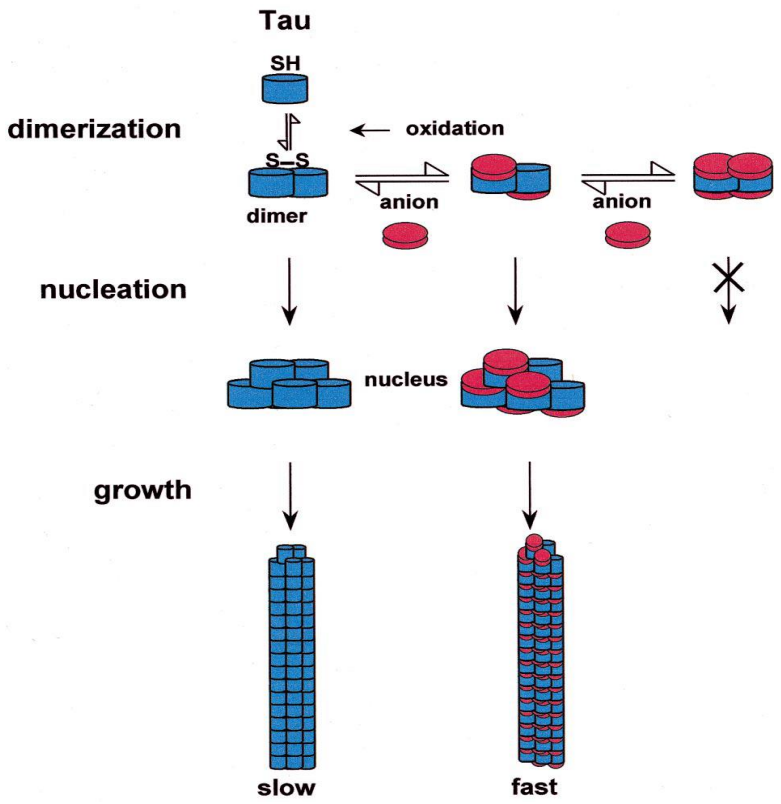

Figure 6: The assembly of tau monomers into dimers, nuclei (oligomers) and paired helical filaments. In *in vitro* experiments, the process may be accelerated by adding a limited amount of anions to the reaction. Dimers may form either via covalent linkage or without (less stable). Source: (Friedhoff et al. 2000). Licenced for reprint under licence number 4112710379685 © Elsevier

Prion-like Spreading

Several proteins associated with neurodegenerative diseases, including tau proteins, amyloid-β and α-synuclein, have been shown to spread in a prion-like manner (Frost and Diamond 2010). If tau protein isolated from human post-mortem tissue is injected into the brains of ALZ17 tau transgenic mice, the tau pathology appears to spread in the same pattern as the original human disease (Clavaguera et al. 2013). The same observation, albeit less dramatic, was made after injecting the extract into wild-type mice. These observations suggest that different tauopathies vary by their pathological conformations and that this conformation can indeed spread in a prion-like self-replicating way. Whilst the mechanism for this spread is still unknown, there have been observations of tau protein trafficking through neuronal membranes and indeed transsynaptically (Dujardin et al. 2014).

Isoform Imbalance

A common classification of tauopathies is between the tauopathies with predominant 3R isoform and the 4R isoform (Chen et al. 2010). While in Alzheimer's disease 3R and 4R isoforms are generally in

balance, there is relatively more 4R isoform tau in PSP, CBD and AGD and in Pick's Disease there is relatively more of the 3R isoform of tau. This imbalance may play a major role in the onset of some tauopathies (Zhou, Yu, and Zou 2008). 4R isoforms are more likely to aggregate than 3R isoforms (Zhou, Yu, and Zou 2008). In fact, a single mutation in the *MAPT* gene encoding the tau protein, affecting only alternative splicing to favour generation of 4R tau, appears to be sufficient to trigger a tauopathy (Spillantini et al. 1998). This has led to the hypothesis that an excess of 4R tau may be deleterious and reducing the relative amount of 4R may be a strategy for a neuroprotective therapy (Avale, Rodriguez-Martin, and Gallo 2013; Zhou, Yu, and Zou 2008). The mechanisms behind the tau isoform balance will be explored further in the first publication enclosed in this dissertation.

Protein kinase R (PKR)-like endoplasmic reticulum kinase (PERK)

The Unfolded Protein Response

PERK is an integral part of the unfolded protein response (UPR), illustrated in Figure 7. The UPR is an evolutionarily conserved mechanism by which the cell responds to stress in the endoplasmic reticulum (ER) to protect the cell's integrity. Stress in the endoplasmic reticulum is triggered by the accumulation of unfolded or misfolded proteins. This may occur in response to changes in the redox environment, Ca^{2+} homeostasis, or energy metabolism (Xu, Bailly-Maitre, and Reed 2005). There are three proteins in the ER membrane sensing ER stress: PERK, endoplasmic reticulum to nucleus signalling 1 (IRE1) and activating transcription factor 6 (ATF6). Their overall downstream effects are to reduce protein synthesis, increase ER folding capacity and to recalibrate the ER environment. This then allows the cell to return to an unstressed state. If, however, the stimulus is severe enough, the mechanism may go into overdrive and apoptosis may be triggered instead.

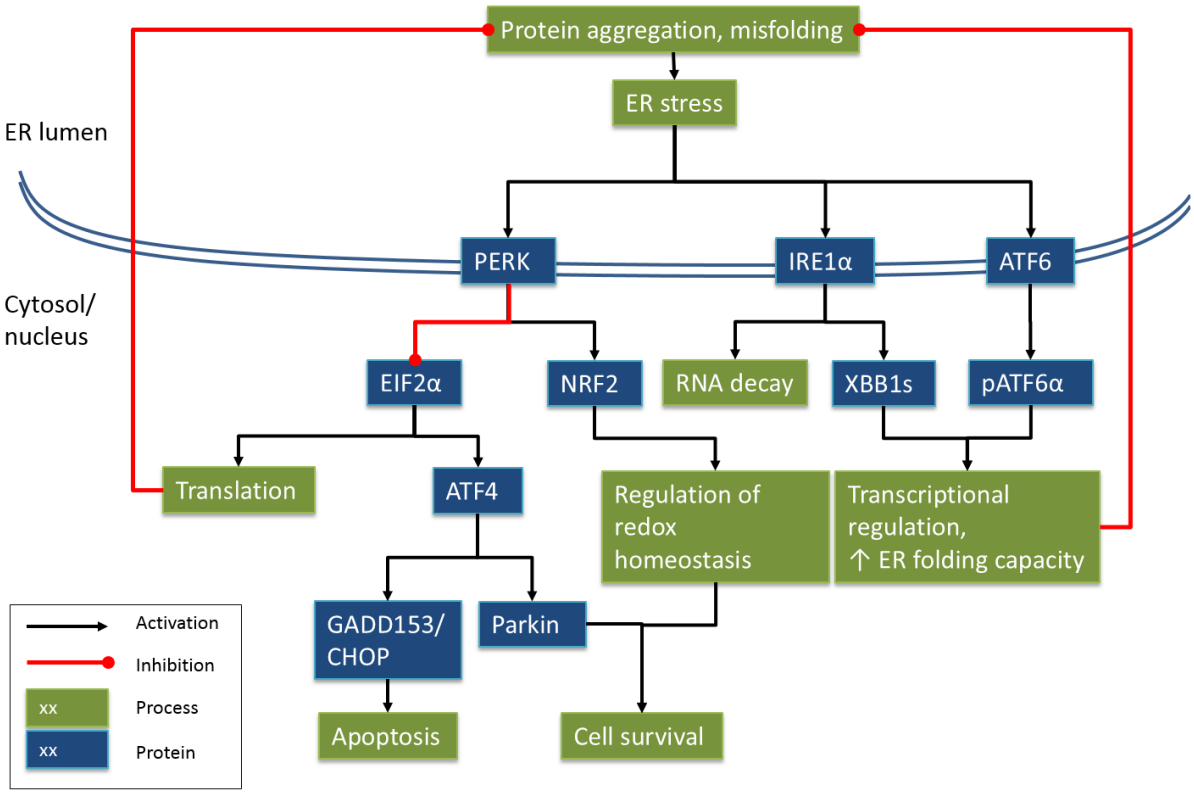

Figure 7: The unfolded protein response and its downstream effects. Own production, modified after Hetz, Martinon et al. 2011.

In the absence of ER stress, the ER chaperone protein binding immunoglobulin protein (BiP) binds to both PERK and IRE1, requiring ATP (Sou, Ilieva, and Polizzi 2012). If an excess of unfolded proteins develops, BiP instead binds to these proteins in the ER lumen. The dissociation of BiP from PERK and the resultant release of energy allows two units of PERK protein to autophosphorylate and dimerise (Bertolotti et al. 2000). This activates the PERK kinase domain.

PERK Signalling

The downstream events of PERK activity are shown in Figure 8. There are two known substrates of PERK kinase activity, the eukaryotic translation initiation factor 2-alpha (EIF2A) and nuclear factor erythroid 2-related factor 2 (NRF2). EIF2A is required for the initiation of translation by ribosomes. Phosphorylation by PERK results in this function being inhibited, whilst also leading to the preferential translation of ATF4, a transcription factor (Blais et al. 2004). Target genes of ATF4 fall into two

categories, depending on the intensity and pattern of the signal (Scheper and Hoozemans 2013; Matsumoto et al. 2013). In response to light stress, parkin (Bouman et al. 2011), a mitochondrial protector, and autophagy (B'Chir et al. 2013; Avivar-Valderas et al. 2011; Vidal and Hetz 2012) are activated. This may protect the cell from any insult caused. If however, the stress signal is strong, suggesting irreversible damage, ATF4 signalling may lead to the induction of apoptosis.

NRF2, on the other hand, is no such double-edged sword. When phosphorylated by PERK it dissociates from its repressor protein Kelch ECH associating protein 1 (KEAP) and translocates into the nucleus (Kansanen et al. 2013). There, it leads to the transcription of genes responsible for oxidative stress protection and cell survival (Cullinan et al. 2003).

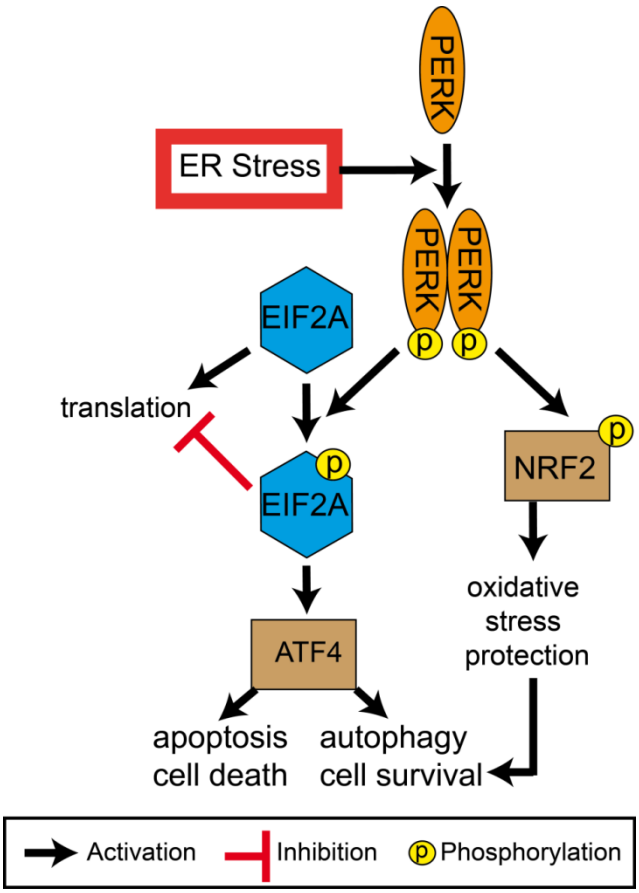

Figure 8: The canonical downstream events of PERK activity. Own production.

PERK Structure

The human PERK protein is made up of 1116 amino acids and three domains – the ER luminal domain, transmembrane domain and the cytosolic domain. The ER luminal domain resides inside the ER lumen, the transmembrane domain anchors the protein to the ER membrane and the cytosolic

domain harbours the kinase active site. In the absence of ER stress PERK is bound to the chaperone protein BiP (Binding immunoglobulin protein). In the presence of ER stress and unfolded proteins, BiP binds to these proteins instead, causing PERK to oligomerise and autophosphorylate (Bertolotti et al. 2000). This is the active state of PERK in which it phosphorylates EIF2A and NRF2.

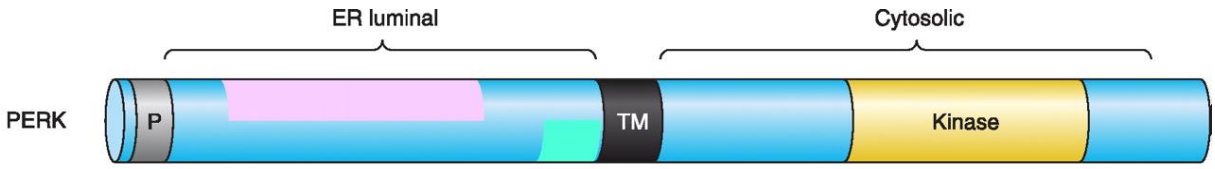

Figure 9: Representation of the structure of the PERK protein. The kinase domain is highlighted in yellow and is frequently the site of mutations or deletions in WRS. TM = transmembrane domain, P = signal sequence, pink shade = BiP interacting domain. Source: Adapted from (Hetz et al. 2011). Published under open source licence © The American Physiological Society

Clinical Implications

PERK therefore plays an important role as a protective mechanism in cells across all organ systems. When it malfunctions, such as in Wolcott Rallison Syndrome (WRS), the results are severe. WRS is a very rare autosomal recessive condition caused by a lack of functional PERK. It is often caused by deletions or mutations in the PERK gene that render the active site inactive. About 60 cases have been described in the literature. The condition is most common in the Middle East, with a fifth coming from Saudi Arabia (Habeb 2013). Most cases are associated with consanguineous marriages. Clinical features are neonatal/early onset skeletal dysplasia and growth retardation, as well as kidney failure, liver failure and microcephaly (Julier and Nicolino 2010). Children born with the condition generally do not reach adulthood.

In addition, PERK has also been implicated in less direct ways in a variety of other diseases, including neurodegenerative diseases (Hetz and Mollereau 2014), cancer, diabetes, autoimmune conditions, liver disorders and obesity (Hetz, Chevet, and Harding 2013).

PERK in Tauopathies

Apart from the genetic association (Hoglinger et al. 2011), there has been experimental evidence for a role of PERK in tauopathies, reviewed e.g. in (Hetz and Mollereau 2014). The increased existence of phosphorylated (i.e. activated) PERK staining in Alzheimer's disease pre-tangle neurons of the

hippocampus was first reported by Hoozemans et al. in 2009 (Hoozemans et al. 2009). UPR activation has also been reported in PSP and Frontotemporal Dementia and Parkinsonism Linked to Chromosome 17 (FTLD-17) (Nijholt et al. 2012; Stutzbach et al. 2013). In PSP, the UPR has been reported to be primarily activated in the pons and medulla and to a lesser extent in the hippocampus (Stutzbach et al. 2013).

These findings have triggered a search for mechanisms of interaction between PERK and tau. Ho et al. (Ho et al. 2012) describe a vicious circle between induced ER-stress and tau-phosphorylation. We also know that PERK activates GSK3ß, one of the tau kinases (Nijholt et al. 2013; Baltzis et al. 2007). Abisambra et al. have found that depleting soluble tau levels in cells and brain could reverse UPR activation (Abisambra et al. 2013) and that soluble tau accumulation impairs the ER-associated protein degradation (ERAD) and this may result in activation of the UPR.

Materials and methods

Methods employed in "Mitochondrial Complex 1 Inhibition Increases 4-Repeat Isoform Tau by SRSF2 Upregulation"

Cell Culture

"Nunc™ Nunclon™ Delta 6-well (for protein and mRNA) or 48-well (for cell assays) plates (Thermo Fisher Scientific, Waltham, MA, USA) were coated with 100 µg/ml poly-L-lysine (Sigma-Aldrich, St. Louis, MO, USA) and 5 µg/ml fibronectin (Sigma-Aldrich). LUHMES (Lund Human Mesencephalic) cells, derived from female human embryonic ventral mesencephalic cells by conditional immortalization (Lotharius et al. 2005) (Tet-off v-myc over-expression) were seeded in a concentration of 130,000 cells /cm^2 to achieve a confluence of 50%. They were then differentiated for 8 days in a medium of DMEM/F12 (Sigma-Aldrich), 1 µg/ml Tetracycline, 2 mg/ml GDNF and 490 µg/ml dbcAMP into post-mitotic neurons (Scholz et al. 2011) with a dopaminergic phenotype (Lotharius et al. 2005). On day 8 post differentiation the cells were treated with 25 nM annonacin, 20 µM 6-OHDA or 10 µM MPP^+ for 48 h. For the intoxication period the medium was replaced with new medium containing glucose levels reduced to 250 µM, i.e. the physiological concentration in the human brain (Silver and Erecinska 1994). For the starving condition, cells were incubated for 24 hours in pure DMEM (Life Technologies, Grand Island, NY, USA) with no additives and no glucose." (Bruch et al. 2014)

Human Brain Tissue and Ethics Statement

"Human fresh frozen brain sections of the *locus coeruleus* area were obtained from The Netherlands Brain Bank, Netherlands Institute for Neuroscience, Amsterdam (www.brainbank.nl). All Material has been collected from donors for or from whom written informed consent for a brain autopsy and the use of the material and clinical information for research purposes had been obtained by The Netherlands Brain Bank in accordance with the Declaration of Helsinki" (Bruch et al. 2014). Table 2 provides an overview of the tissue samples used.

Table 2: Overview of Human Tissue Used (Bruch et al. 2014)

Case Number	Diagnosis	Cause of Death	Age at death	Braak Stage	Sex	Postmortem delay (hours:minutes)
P1	PSP	"Natural death"	73	2C	Male	4:20
P2	PSP	Acute heart failure	70	3	Male	6:50
P3	PSP	Aspiration pneumonia	73	2	Male	6:15
P4	PSP	Urinary tract infection	70	1A	Male	5:20
C1	Non-demented control	Pancreas carcinoma	70	0	Male	7:30
C2	Non-demented control	Prostate cancer	69	0	Male	5:55
C3	Non-demented control	Lung emboli (clinical suspicion)	73	0	Male	24:45
C4	Non-demented control	Sepsis	71	1	Male	7:40
C5	Non-demented control	Myocardial infarction	67	1B	Male	18:35

Quantitative Real-Time PCR

"RNA from human tissue samples was extracted by grinding the tissue in liquid nitrogen to a powder and then dissolving it in the RA1 buffer supplied as part of the NucleoSpin® RNA (Macherey Nagel, Düren, Germany) RNA extraction kit + 1 % (v/v) 2-Mercaptoethanol (Sigma-Aldrich). RNA from cells was extracted by scraping the cells from the culture plate with RA1 buffer + 1 % (v/v) 2-Mercaptoethanol. The remaining extraction procedure was according to the manufacturer's instructions for the NucleoSpin® RNA kit. RNA concentrations were determined using the NanoDrop 2000c Spectrophotometer (Thermo Fisher Scientific). The RNA was then transcribed into cDNA with the iScript™ cDNA Synthesis Kit (BioRad, Berkeley, CA, USA) using the manufacturer's instructions. Real-Time PCR was performed on the Applied Biosystems® StepOnePlus™ (Life Technologies) system using TaqMan® Universal Master Mix II and TaqMan® primers against total *MAPT, MAPT 0N, MAPT 1N, MAPT 2N, MAPT 3R, MAPT 4R, SRSF1, SRSF2, SRSF3, SRSF6, SRSF7, SRSF9, SRSF11* and *TRA2B*. *PSMC1* and *POL2A* were used as reference genes for relative quantification in all tau splicing factor experiments, while *PPIB* and *GAPDH* were used in all tau isoform experiments as they were determined to be the most stably expressed across the respective experimental conditions. All values are relative quantities compared to untreated (control) cells. Three biological repeats with three technical repeats each were analysed. Analysis was conducted with the Applied Biosystems® StepOnePlus™ (Life Technologies) and Qbase+ (Biogazelle, Zwijnaarde, Belgium) software packages. Absolute quantification was performed by creating a standard curve with plasmids containing either

the 2N3R or the 2N4R spliced variant of *MAPT* (obtained as a gift from Eva-Maria Mandelkow, DZNE Bonn, Germany). The absolute quantity was computed by deriving the relationship between CT values and absolute quantity with the StepOne Plus software." (Bruch et al. 2014)

Western Blotting

"Protein was extracted from cells using the M-PER Mammalian Protein Extraction Reagent (Thermo Fisher Scientific). The protein solution was frozen at -80°C immediately after retrieval and for a minimum of two hours. The solution was then thawed on ice, vortexed, centrifuged at 5000 g for 15 minutes at 4°C and the supernatant retrieved. Total protein concentrations were determined using the BCA kit (Thermo Fisher Scientific) by heating the samples at 60°C for 30 minutes and measuring the absorption on the NanoDrop 2000c Spectrophotometer (Thermo Fisher Scientific). 20 µg of total protein were then adjusted to equal concentrations between samples by dilution with M-PER and subsequently heated at 95°C for 5 minutes with Roti®-Load 1 (Carl Roth, Karlsruhe, Germany). SDS-PAGE was performed using Any kD™ Mini-PROTEAN® TGX™ Gels (Bio-Rad) in a tris-glycine running buffer (14.4% glycine, 3% Tris, 1% SDS w/v, Carl Roth). The protein was blotted onto PVDF membrane (Bio-Rad) at 70 V for 65 minutes. The membrane was blocked with 1 x Roti®-Block solution (Carl Roth) for 1h and then incubated at 4°C overnight under gentle shaking with the primary antibody (see Table 3) in TBS with 5% BSA (Cell Signaling, Danvers, MA, USA) and 0.05% TWEEN (Sigma-Aldrich). The membranes were then washed and incubated with the appropriate secondary antibody at 1:2500 (v/v) in 1 x Roti®-Block solution for 2h, followed by further washing and exposure to Clarity Western ECL Substrate (Bio-Rad) or, in the case of 4-repeat tau, to Amersham™ *ECL™ Prime* (General Electric, Fairfield, CT, USA). Chemiluminescence was detected with the Gel Doc™ XR System (Bio-Rad) and analysed by background subtracted optical density analysis with Image Lab™ software (Bio-Rad)." (Bruch et al. 2014)

Table 3: Primary Antibody Concentrations Used (Bruch et al. 2014)

Antigen	Clone	Species	Concentration (v/v)	Company
Human tau	HT7	Mouse	1:1000	Pierce Antibodies, Thermo
3-repeat tau	8E6/C11	Mouse	1:500	Millipore
4-repeat tau	1E1/A6	Mouse	1:300	Millipore
Actin (I-19)	Polyclonal	Goat	1:2500	Santa Cruz Biotechnologies

siRNA Silencing

"LUHMES cells were seeded out and differentiated as described above and allowed to adhere to the plate floor for 4 h. MISSION® esiRNA (Sigma-Aldrich) targeted against SRSF2 (final concentration 200 nM) and Lipofectamine® RNAiMAX (Life Technologies) (final concentration 1.2 µl/ml) were dissolved

in separate aliquots of OptiMEM® (Life Technologies). The diluted esiRNA was then added to the diluted Lipofectamine® RNAiMAX. The combined solution was then allowed to incubate for 20 minutes before being added to the cells." (Bruch et al. 2014)

ATP Assay

"ATP assays were conducted using the ViaLight™ plus kit by Lonza according to the manufacturer's instructions. Luminescence was read with the FLUOstar Omega (BMG Labtech) platereader. The data was analysed using the MARS Data Analysis Software (BMG Labtech)." (Bruch et al. 2014)

MTT Assay

"Thiazolyl Blue Tetrazolium Blue (MTT) (Sigma Aldrich) was dissolved in sterile PBS to a concentration of 5 mg/ml. This stock solution was added to the cells in culture medium to achieve a final concentration of 0.5 mg/ml. The 48-well culture plate was then incubated at 37°C for 1 h, the medium removed completely and frozen at -80°C for 1 h. The plate was then thawed, 300 µl DMSO (AppliChem, Darmstadt, Germany) was added per well and the plate was shaken to ensure complete dissolution of the violet crystals. 100 µl from each well were transferred to a new 96-well plate and the absorbance was read with the FLUOstar Omega (BMG Labtech) platereader at a wavelength of 590 nm (reference wave length 630 nm). The data was analysed using the MARS Data Analysis Software (BMG Labtech)." (Bruch et al. 2014)

Statistics

"Prism 6 (GraphPad Software, La Jolla, CA, USA) was used for statistical calculations and for the creation of line and bar graphs. Results were compared by 2-way ANOVA with Sidak post-hoc test, unless stated otherwise. Data are shown as mean ± SEM. $P < 0.05$ was considered significant." (Bruch et al. 2014)

Methods employed in "Early Neurodegeneration in the Brain of a Child Without Functional PKR-like Endoplasmic Reticulum Kinase"

Search for Human Postmortem Tissue

"We started our search for WRS postmortem brain material by contacting all institutions that had published cases of the syndrome or written about the syndrome in the pubmed-listed literature. This step yielded samples of one patient from Lyon University Paediatric Hospital, Lyon, France, in which EIF2AK3 had previously been identified as the gene responsible for WRS. In the next step, we searched the BrainNet Europe database and contacted leading paediatric units across the world.

However, we were unable to find brain material from further WRS cases with confirmed *EIF2AK3* mutations." (Bruch et al. 2015)

Genotyping

"DNA was extracted from peripheral blood collected on EDTA. WRS was confirmed by direct sequencing of EIF2AK3 on genomic DNA as previously described (5), which showed a c.3009C>T substitution homozygous in the patient and heterozygous in the parents, resulting in a p.R903* nonsense mutation and a truncated protein." (Bruch et al. 2015)

Human Postmortem Tissue

"Three blocks (2 x frontal cortex, 1 x cerebellum) of paraffin embedded tissue from a single patient were obtained from the Department of Pathology and Neuropathology, Groupement Hospitalier Est, Bron, France. The parents had given full permission for use of the material and medical records for research purposes according to the Declaration of Helsinki. Equivalent blocks of paraffin-embedded tissue from three age-matched control cases were obtained from the Center for Neuropathology and Prion Research (ZNP), University of Munich, Munich, Germany. They were anonymised routine biopsy cases. Usage of the material was in accordance with the directives of the local ethics commission regarding the use of archive material for research purposes" (Bruch et al. 2015). Table 4 shows an overview of the cases used.

Table 4: Overview over the human tissue used (Bruch et al. 2015)

Case Number	Diagnosis	Cause of Death	Age at death	Sex	Postmortem delay
WRS	Wolcott Rallison Syndrome	Hepatic and renal failure	4	m	unknown
C1	Control	Pulmonary hypertension	3	m	48 h
C2	Control	Aplastic anaemia	6.5	m	24 h
C3	Control	Pneumonia	4	m	65 h

Immunohistochemistry

"The paraffin blocks were cut on a microtome to a thickness of 5 µm. The tissue was deparaffinised and progressively rehydrated according to the Abcam protocol (www.abcam.com/protocols). Haematoxylin and Eosin (H+E; Hoffmann-LaRoche, Basel, Switzerland) staining was performed according to the manufacturer's guidelines. Antigen retrieval was done by heating the slides in 10 mM sodium citrate (Sigma-Aldrich, St. Louis, MO, USA) buffer at 90°C for 20 minutes. All immunohistochemical stainings were performed semi-automatically on a BenchMark IHC device

(Ventana, now Hoffmann-LaRoche). The primary antibodies, concentrations and incubation times used are shown in Table 5. iView DAB and ultraView DAB were used as detection systems. Nuclear counterstaining was done with haematoxylin (Hoffmann-LaRoche). Microscopy and imaging were performed on a Leica CTR 6000 microscope (Leica Microsystems, Wetzlar, Germany)." (Bruch et al. 2015)

Double Label Immunofluorescence

"The tissue sections were cut, deparaffinised, rehydrated and antigens retrieved as above. The slides were blocked in 5% normal goat serum (NGS, Vector Laboratories, Burlingame, CA, USA) in PBS with 0.2% TWEEN (Sigma-Aldrich, St. Louis, MO, USA). Primary antibody incubation was in 2% NGS in PBST overnight at 4°C. Antibodies and concentrations used are listed in Table 5. The slides were washed 3 x for 5 minutes in PBS and then incubated for two hours in 2% NGS in PBST at room temperature with the fluorescent secondary antibodies Alexa Fluor® 488 Goat Anti-Mouse IgG (Life Technologies, now Thermo-Fisher Scientific, Carlsbad, CA, USA) and Alexa Fluor® 594 Goat Anti-Rabbit IgG (Life Technologies). DAPI dihydrochloride (Thermo-Fisher Scientific) was added at 300 nM and incubated for 10 minutes. The slides were washed 3 x 5 minutes in PBS and then coverslipped with polyvinyl alcohol mounting medium with DABCO® anti-fading mounting medium (Sigma-Aldrich). Microscopy and imaging were performed on a Leica TCS SP5 II laser confocal microscope (Leica Microsystems)." (Bruch et al. 2015)

Table 5: Overview of the primary antibodies and concentrations used. RT = room temperature (Bruch et al. 2015)

Antigen	Clone	Species	Incubation Time and temperature	Concentration	Detection System	Source
PHF tau	AT8	Mouse	1 h, RT	1:200	iView DAB	Themo-Fisher Scientific
GFAP	GA5	Mouse	1 h, RT	1:100	iView DAB	Cell Signaling
p62 Lck Ligand	3	Mouse	1 h, RT	1:100	iView DAB	BD Biosciences
Ubiquitin	polyclonal	Rabbit	Overnight, 4°C	1:100	Fluorescence	Abcam
Cleaved caspase 3	D3E9	Rabbit	Overnight, 4°C	1:100	iView DAB	Cell Signalling
NeuN	polyclonal	Rabbit	Overnight, 4°C	1:200	iView DAB	EMD Millipore
Alpha-synuclein	42	Mouse	1 h, RT	1:2000	ultraView DAB	BD Biosciences
LC3B	D11	Rabbit	Overnight, 4°C	1:100	Fluorescence	Cell Signaling
FUS	polyclonal	Rabbit	1 h, RT	1:100	ultraView DAB	Bethyl Laboratories
pTDP-43	polyclonal	Rat	1 h, RT	1:50	ultraView DAB	Own production by cooperation partner
Beta Amyloid	6E10	Mouse	1h, RT	1:2000	iView DAB	Covance
Microglial NP_001614 and NP_116573	Iba1	Rabbit	1h, RT	1:500	iView DAB, microwave pretreat-ment	Wako
Activated microglia	CR3/43	Mouse	1h, RT	1:100	iView DAB	Dako

Summaries of enclosed publications

Summary of the publication „Mitochondrial Complex 1 Inhibition Increases 4-Repeat Isoform Tau by SRSF2 Upregulation“

Background

Tauopathies are a group of neurodegenerative diseases characterized by the intracellular aggregation of tau protein. Alternative splicing of the tau gene *MAPT* (mictotubule associated protein tau) leads to the creation of 6 predominant isoforms. Depending on the inclusion or exclusion of exon 10, tau protein has either 3 (3R-tau) or 4 (4R-tau) microtubule binding sites. While the 3R and 4R isoforms are usually in balance, in PSP, there is an excess of the 4R isoforms. This imbalance is thought to contribute significantly to the pathology of PSP. Yet, so far no reason for the 4R increase has been identified. Exon 10 alternative splicing is controlled both by cis-elements in exon 10 and intron 10, as well as by transacting factors, such as a group of proteins called splicing factors which modify the action of the spliceosome in alternative splicing. Annonacin is a mitochondrial complex I inhibitor naturally occurring in some fruit and with a strong epidemiological link to a PSP-like tauopathy. As annonacin treatment results in changes suggestive of tauopathy in cell culture it serves as a suitable model for PSP.

Results

When human neurons were exposed to annonacin, 4R-tau became upregulated both on the protein level, as detected by Western blot, and the mRNA level, as detected by qPCR. There was no other significant change in alternative splicing although there was a slight increase in 0N isoforms. All splicing factors known to influence the alternative splicing of exon 10 were analysed for their reaction to annonacin. Only SRSF2 was significantly upregulated by annonacin. siRNA mediated knockdown of SRSF2 virtually eliminated this effect, suggesting that SRSF2 is a necessary intermediary for annonacin induced 4R upregulation. The same effect as annonacin was also seen with MPP+, another mitochondrial complex I inhibitor. 6-OHDA, a neurotoxin which exerts its toxicity primarily by oxidative stress and starvation, on the other hand, did not cause any 4R tau upregulation. This suggests that 4R upregulation is common to all toxins inhibiting complex I but not to those toxins interfering with respiration more generally. SRSF2 was also found to be elevated in brain tissue samples of PSP patients compared to non-demented controls. However, in addition the splicing factor TRB2B was also elevated. This suggests that 4R upregulation in human PSP can be partially explained by complex 1 inhibition, however, an additional TRB2B mediated mechanism also seems to play a role.

Discussion

This paper adds three key insights: First, annonacin models the isoform imbalance seen in some forms of tauopathy such as PSP. Second, SRSF2 is a splicing factor that is essential for complex I mediated 4R tau upregulation. Finally, mitochondrial complex 1 inhibition can explain part of the 4R-tau upregulation seen in PSP, however, an additional TRB2B mediated mechanism may also play a role.

Own contributions

I wrote the manuscript and performed all experiments on the human brain tissue and on the cell cultures relating to splicing factors and annonacin. I also organized the human brain tissue samples from the Netherlands Brain Bank. Hong Xu performed the experiments relating to the other toxins.

Summary of the publication „Early Neurodegeneration in the Brain of a Child Without Functional PKR-like Endoplasmic Reticulum Kinase“

Background

Wolcott Rallison Syndrome (WRS) is the very rare clinical manifestation of a lack of functional PKR-like Endoplasmic Reticulum Kinase (PERK). PERK is one of the key effector signalling proteins in the unfolded protein response (UPR), a natural cellular response to ER stress, such as an overload of misfolded proteins. The syndrome is autosomal recessive and characterized by infancy-onset diabetes mellitus, multiple epiphyseal dysplasia, osteopenia, microcephaly and mental retardation. PERK has recently been implicated in the pathogenesis of several neurodegenerative conditions, such as Alzheimer disease, other tauopathies, and Parkinson disease. However, there has never previously been a neuropathological study of a WRS patient been described in the literature.

Results

There are about 60 cases of Wolcott Rallison Syndrome described in the literature. An extensive global search for brain tissue of PERK patients, based first on publications and then on known brain banks and leading institutions, resulted in only one existing tissue sample being identified. It was paraffin embedded tissue blocks of the cerebellum and frontal cortex of a four year old child from Lyon University Pediatric Hospital. Age matched control brains were taken from the brain bank at the Center for Neuropathology and Prion Research, University of Munich.

The brain showed no obvious macroscopic abnormality apart from being slightly oedematous with tonsillar herniation. Sections had a pale appearance. Hematoxylin and eosin stainings showed reduced cell density in the molecular layer of the cerebellum and the outer gray matter layers of the frontal cortex in the WRS case compared with age matched controls. GFAP staining showed thickened and corkscrew like Bergmann glia and clusters of reactive astrocytes. The microglial marker Iba1 showed increased density and clustering of microglia. Staining for the paired helical filament tau marker AT8 revealed the presence of neurofibrillary tangles in the cytoplasm of some neurons – a feature generally associated with some tauopathies such as PSP. There were neurons positive for FUS – associated with certain types of frontotemporal dementia. Additional cells stained positive for p62 and there was colocalization of p62 with ubiquitin and LC3 on laser confocal microscopy. This suggests impaired autophagic flux, a further feature associated with several neurodegenerative diseases.

Discussion

The role of PERK and the unfolded protein response in the pathogenesis of tauopathies and other neurodegenerative conditions has been subject to recent debate. The neuropathological examination presented a unique opportunity to gain insight into PERK function in the human brain without the limitations of animal models or cell cultures. The key insight gained is that a lack of functional PERK is sufficient to induce early signs of neurodegenerative diseases. This is highly relevant as so far there is no consensus in the literature on whether the UPR is beneficial or harmful in the pathogenesis of neurodegenerative conditions. Furthermore, the findings confirm the importance of PERK for autophagy in the pathogenesis of neurodegeneration.

Own contributions

I coordinated the whole study, searched for possible tissue samples and control tissues, performed some of the immunohistochemical stainings and all of the double label immunohistochemistry stainings, took the photographs, performed the data analysis and wrote the manuscript.

Discussion

The journey of discovering the link between the protein PERK and the tauopathy PSP was initiated by the discovery of a genetic association between the two as part of a GWAS (Hoglinger et al. 2011). My work has subsequently focused on exploring the functional biological basis of this association.

Bruch et al. 2015 represents a first step towards this by exploring the effect of the absence of PERK, which is commonly undertaken as first step towards exploring the function of a protein. In the case of PERK, both general (Zhang et al. 2002) knockout and brain-specific disruption (Trinh et al. 2012) models have already been created in mice. However, the examination of a human brain without functional PERK was a unique opportunity to explore the effects of PERK without the constraints of animal models (mice, for example, have significant differences in the PERK and tau protein structure compared to humans) and over an extended period of time (the patient examined in our study lived for four years) (Bruch et al. 2015).

Bruch et al. 2014 may be regarded as a further step in the process of investigating the relationship between PERK and PSP. The imbalance of tau isoforms in PSP in favor of 4R tau (Zhou, Yu, and Zou 2008; Bruch et al. 2014) is thought to play a significant role in the pathogenesis of PSP. Therefore, a model is required to study the effects on isoform imbalance. Bruch et al. 2014 shows that annonacin intoxication of cultured cells provides such a model. It also shows that SRSF2 is a splicing factor linking mitochondrial complex I inhibition with the increase in 4R tau isoforms and that levels of this splicing factor are elevated in PSP, together with one other splicing factor – TRA2B.

Further insights into the impact of PERK in PSP were subsequently gained through pharmacological activation and inhibition of PERK (Bruch et al. 2017; Radford et al. 2015). In Bruch et al. 2017 we were able to show that PERK activation abolishes the SRSF2 dependent increase in 4R tau and therefore seems to play a role in tau isoform balance control via SRSF2. In addition, PERK activation also reduced many stigmata of tau pathology both *in vitro* and *in vivo* – including tau phosphorylation, conformational change, neuronal cell viability, as well as memory function and motor function in the common P301S tau mouse model for PSP. Recently, there has been suggestion of a vicious cycle between tau pathology and oxidative stress at the core of tauopathy pathogenesis (Alavi Naini and Soussi-Yanicostas 2015). As the PERK substrate NRF2 is a key player in the mitigation of oxidative stress and PERK reduces SRSF2 mediated 4R tau imbalance, PERK could play a central role in breaking such a vicious circle.

There are, however, a couple of factors which qualify the significance of the findings described in this thesis. For example, those experiments relying on human tissue had to be conducted with very limited sample numbers. Especially in the case of the neuropathological study of a human case of Wollcott Rallison Syndrome it was only possible to examine a single case due to brain tissue generally not having been preserved from autopsies. The examined case's cause of death was also secondary to multi-organ failure which may have affected the pathology – although this is the changes observed are unlikely to have come on acutely. Also for the examination of splicing factor and tau isoform levels we were only able to obtain 4 PSP and 5 control cases, although in this case results were statistically significant and - in the case of isoform levels - are backed by prior studies (Buee and Delacourte 1999; Dickson et al. 2011).

The human brain samples used also partly had extensive post mortem delay times – in one case up to 65 hours. Santpere et al. 2006 found that tau degradation, manifested as a reduction in the number and intensity of bands, may occur between 8 and 26 h post-mortem and is universal in samples with post-mortem delays of 50h (Santpere, Puig, and Ferrer 2006). However, similar studies have compared the effects between diseases at different post mortem delays and found the results still to hold even after long delays (Wiersma et al. 2016).

The studies using annonacin as a model for PSP rely heavily on the theory that PSP can be caused by environmental factors. Most evidence, however, points towards both environmental and genetic factors playing a role in the pathogenesis of most cases of PSP (Alavi Naini and Soussi-Yanicostas 2015). Annonacin, therefore only models one part of the putative PSP pathogenesis. This could, for example, be one reason why the splicing factor TRA2B is increased in PSP even though annonacin does not have an effect on it in the *in vitro* models studied (Bruch et al. 2014). However, the significance of the isoform balance for the pathogenesis of PSP also still needs to be established more firmly. Whilst an increase in 4R tau alone is sufficient to trigger a tauopathy (Spillantini et al. 1998), there is also evidence that 4R isoform imbalance may only occur in certain parts of the brain of PSP patients while in other parts the same stigmata of PSP are evident without an increase in 4R isoform tau (Chambers et al. 1999) . An interesting question is also why tau protein is responsible for such a wide spectrum of different neurodegenerative diseases with the tau aggregates in PSP being of different shape and distribution than in other 4R tauopathies such as argyrophilic grain disease (AGD). This variation could be related to different environmental and genetic factors acting through pathways downstream of mitochondrial complex I – but this needs to be explored further.

What should also be explored further is the relevance of the findings to other neurodegenerative diseases. The research has mainly focused on PSP and models for PSP because of the genetic

association between PERK and PSP. However, as ER stress has been identified in many neurodegenerative diseases (Hetz and Mollereau 2014), it is possible that similar mechanisms are also relevant for other tauopathies, as well as other protein aggregating neurodegenerative diseases.

The activation of PERK as a form of therapy to mitigate tau pathology is in the patent application process (patent WO 2016024010 A1) and is currently being investigated further for safety and efficacy.

References

Abisambra, J. F., U. K. Jinwal, L. J. Blair, J. C. O'Leary, 3rd, Q. Li, S. Brady, L. Wang, C. E. Guidi, B. Zhang, B. A. Nordhues, M. Cockman, A. Suntharalingham, P. Li, Y. Jin, C. A. Atkins, and C. A. Dickey. 2013. 'Tau accumulation activates the unfolded protein response by impairing endoplasmic reticulum-associated degradation', *J Neurosci*, 33: 9498-507.

Alavi Naini, S. M., and N. Soussi-Yanicostas. 2015. 'Tau Hyperphosphorylation and Oxidative Stress, a Critical Vicious Circle in Neurodegenerative Tauopathies?', *Oxid Med Cell Longev*, 2015: 151979.

Aldrich, M. S., N. L. Foster, R. F. White, L. Bluemlein, and G. Prokopowicz. 1989. 'Sleep abnormalities in progressive supranuclear palsy', *Ann Neurol*, 25: 577-81.

Avale, M. E., T. Rodriguez-Martin, and J. M. Gallo. 2013. 'Trans-splicing correction of tau isoform imbalance in a mouse model of tau mis-splicing', *Hum Mol Genet*, 22: 2603-11.

Avivar-Valderas, A., E. Salas, E. Bobrovnikova-Marjon, J. A. Diehl, C. Nagi, J. Debnath, and J. A. Aguirre-Ghiso. 2011. 'PERK integrates autophagy and oxidative stress responses to promote survival during extracellular matrix detachment', *Mol Cell Biol*, 31: 3616-29.

B'Chir, W., A. C. Maurin, V. Carraro, J. Averous, C. Jousse, Y. Muranishi, L. Parry, G. Stepien, P. Fafournoux, and A. Bruhat. 2013. 'The eIF2alpha/ATF4 pathway is essential for stress-induced autophagy gene expression', *Nucleic Acids Res*, 41: 7683-99.

Baltzis, D., O. Pluquet, A. I. Papadakis, S. Kazemi, L. K. Qu, and A. E. Koromilas. 2007. 'The eIF2alpha kinases PERK and PKR activate glycogen synthase kinase 3 to promote the proteasomal degradation of p53', *J Biol Chem*, 282: 31675-87.

Battisti, A., G. Ciasca, and A. Tenenbaum. 2013. 'Transient tertiary structures in tau, an intrinsically disordered protein', *Molecular Simulation*, 39: 1084-92.

Bertolotti, A., Y. Zhang, L. M. Hendershot, H. P. Harding, and D. Ron. 2000. 'Dynamic interaction of BiP and ER stress transducers in the unfolded-protein response', *Nat Cell Biol*, 2: 326-32.

Biernat, J., N. Gustke, G. Drewes, E. M. Mandelkow, and E. Mandelkow. 1993. 'Phosphorylation of Ser262 strongly reduces binding of tau to microtubules: distinction between PHF-like immunoreactivity and microtubule binding', *Neuron*, 11: 153-63.

Billingsley, M. L., and R. L. Kincaid. 1997. 'Regulated phosphorylation and dephosphorylation of tau protein: Effects on microtubule interaction, intracellular trafficking and neurodegeneration', *Biochemical Journal*, 323: 577-91.

Blais, J. D., V. Filipenko, M. Bi, H. P. Harding, D. Ron, C. Koumenis, B. G. Wouters, and J. C. Bell. 2004. 'Activating transcription factor 4 is translationally regulated by hypoxic stress', *Mol Cell Biol*, 24: 7469-82.

Bouman, L., A. Schlierf, A. K. Lutz, J. Shan, A. Deinlein, J. Kast, Z. Galehdar, V. Palmisano, N. Patenge, D. Berg, T. Gasser, R. Augustin, D. Trumbach, I. Irrcher, D. S. Park, W. Wurst, M. S. Kilberg, J. Tatzelt, and K. F. Winklhofer. 2011. 'Parkin is transcriptionally regulated by ATF4: evidence for an interconnection between mitochondrial stress and ER stress', *Cell Death Differ*, 18: 769-82.

Bruch, J., C. Kurz, A. Vasiljevic, M. Nicolino, T. Arzberger, and G. U. Hoglinger. 2015. 'Early Neurodegeneration in the Brain of a Child Without Functional PKR-like Endoplasmic Reticulum Kinase', *J Neuropathol Exp Neurol*, 74: 850-7.

Bruch, J., H. Xu, A. De Andrade, and G. Hoglinger. 2014. 'Mitochondrial complex 1 inhibition increases 4-repeat isoform tau by SRSF2 upregulation', *PLoS One*, 9: e113070.

Bruch, J., H. Xu, T. W. Rosler, A. De Andrade, P. H. Kuhn, S. F. Lichtenthaler, T. Arzberger, K. F. Winklhofer, U. Muller, and G. U. Hoglinger. 2017. 'PERK activation mitigates tau pathology in vitro and in vivo', *EMBO Mol Med*, 9: 371-84.

Brunden, K. R., J. Q. Trojanowski, and V. M. Lee. 2009. 'Advances in tau-focused drug discovery for Alzheimer's disease and related tauopathies', *Nat Rev Drug Discov*, 8: 783-93.

Buee, L., and A. Delacourte. 1999. 'Comparative biochemistry of tau in progressive supranuclear palsy, corticobasal degeneration, FTDP-17 and Pick's disease', *Brain Pathol*, 9: 681-93.

Cairns, N. J., V. M. Lee, and J. Q. Trojanowski. 2004. 'The cytoskeleton in neurodegenerative diseases', *J Pathol*, 204: 438-49.

Chambers, C. B., J. M. Lee, J. C. Troncoso, S. Reich, and N. A. Muma. 1999. 'Overexpression of four-repeat tau mRNA isoforms in progressive supranuclear palsy but not in Alzheimer's disease', *Ann Neurol*, 46: 325-32.

Chen, S., K. Townsend, T. E. Goldberg, P. Davies, and C. Conejero-Goldberg. 2010. 'MAPT isoforms: differential transcriptional profiles related to 3R and 4R splice variants', *J Alzheimers Dis*, 22: 1313-29.

Clavaguera, F., H. Akatsu, G. Fraser, R. A. Crowther, S. Frank, J. Hench, A. Probst, D. T. Winkler, J. Reichwald, M. Staufenbiel, B. Ghetti, M. Goedert, and M. Tolnay. 2013. 'Brain homogenates from human tauopathies induce tau inclusions in mouse brain', *Proc Natl Acad Sci U S A*, 110: 9535-40.

Cullinan, S. B., D. Zhang, M. Hannink, E. Arvisais, R. J. Kaufman, and J. A. Diehl. 2003. 'Nrf2 is a direct PERK substrate and effector of PERK-dependent cell survival', *Mol Cell Biol*, 23: 7198-209.

Dickson, D. W., N. Kouri, M. E. Murray, and K. A. Josephs. 2011. 'Neuropathology of frontotemporal lobar degeneration-tau (FTLD-tau)', *J Mol Neurosci*, 45: 384-9.

Donker Kaat, L., A. J. Boon, A. Azmani, W. Kamphorst, M. M. Breteler, B. Anar, P. Heutink, and J. C. van Swieten. 2009. 'Familial aggregation of parkinsonism in progressive supranuclear palsy', *Neurology*, 73: 98-105.

Dujardin, S., K. Lecolle, R. Caillierez, S. Begard, N. Zommer, C. Lachaud, S. Carrier, N. Dufour, G. Auregan, J. Winderickx, P. Hantraye, N. Deglon, M. Colin, and L. Buee. 2014. 'Neuron-to-neuron wild-type Tau protein transfer through a trans-synaptic mechanism: relevance to sporadic tauopathies', *Acta Neuropathol Commun*, 2: 14.

Escobar-Khondiker, M., M. Hollerhage, M. P. Muriel, P. Champy, A. Bach, C. Depienne, G. Respondek, E. S. Yamada, A. Lannuzel, T. Yagi, E. C. Hirsch, W. H. Oertel, R. Jacob, P. P. Michel, M. Ruberg, and G. U. Hoglinger. 2007. 'Annonacin, a natural mitochondrial complex I inhibitor, causes tau pathology in cultured neurons', *J Neurosci*, 27: 7827-37.

Friedhoff, P., M. von Bergen, E. M. Mandelkow, and E. Mandelkow. 2000. 'Structure of tau protein and assembly into paired helical filaments', *Biochim Biophys Acta*, 1502: 122-32.

Frost, B., and M. I. Diamond. 2010. 'Prion-like mechanisms in neurodegenerative diseases', *Nat Rev Neurosci*, 11: 155-9.

Goedert, M., M. G. Spillantini, R. Jakes, D. Rutherford, and R. A. Crowther. 1989. 'Multiple Isoforms of Human Microtubule-Associated Protein-Tau - Sequences and Localization in Neurofibrillary Tangles of Alzheimers-Disease', *Neuron*, 3: 519-26.

Goetz, C. G. 1996. 'An early photographic case of probable progressive supranuclear palsy', *Mov Disord*, 11: 617-8.

Habeb, A. M. 2013. 'Frequency and spectrum of Wolcott-Rallison syndrome in Saudi Arabia: a systematic review', *Libyan J Med*, 8: 21137.

Hasegawa, M., R. A. Crowther, R. Jakes, and M. Goedert. 1997. 'Alzheimer-like changes in microtubule-associated protein Tau induced by sulfated glycosaminoglycans. Inhibition of microtubule binding, stimulation of phosphorylation, and filament assembly depend on the degree of sulfation', *J Biol Chem*, 272: 33118-24.

Hauw, J. J., S. E. Daniel, D. Dickson, D. S. Horoupian, K. Jellinger, P. L. Lantos, A. McKee, M. Tabaton, and I. Litvan. 1994. 'Preliminary NINDS neuropathologic criteria for Steele-Richardson-Olszewski syndrome (progressive supranuclear palsy)', *Neurology*, 44: 2015-9.

Hetz, C., E. Chevet, and H. P. Harding. 2013. 'Targeting the unfolded protein response in disease', *Nat Rev Drug Discov*, 12: 703-19.

Hetz, C., F. Martinon, D. Rodriguez, and L. H. Glimcher. 2011. 'The unfolded protein response: integrating stress signals through the stress sensor IRE1alpha', *Physiol Rev*, 91: 1219-43.

Hetz, C., and B. Mollereau. 2014. 'Disturbance of endoplasmic reticulum proteostasis in neurodegenerative diseases', *Nat Rev Neurosci*, 15: 233-49.

Ho, Y. S., X. Yang, J. C. Lau, C. H. Hung, S. Wuwongse, Q. Zhang, J. Wang, L. Baum, K. F. So, and R. C. Chang. 2012. 'Endoplasmic reticulum stress induces tau pathology and forms a vicious cycle: implication in Alzheimer's disease pathogenesis', *J Alzheimers Dis*, 28: 839-54.

Hoglinger, G. U., N. M. Melhem, D. W. Dickson, P. M. Sleiman, L. S. Wang, L. Klei, R. Rademakers, R. de Silva, I. Litvan, D. E. Riley, J. C. van Swieten, P. Heutink, Z. K. Wszolek, R. J. Uitti, J. Vandrovcova, H. I. Hurtig, R. G. Gross, W. Maetzler, S. Goldwurm, E. Tolosa, B. Borroni, P. Pastor, P. S. P. Genetics Study Group, L. B. Cantwell, M. R. Han, A. Dillman, M. P. van der Brug, J. R. Gibbs, M. R. Cookson, D. G. Hernandez, A. B. Singleton, M. J. Farrer, C. E. Yu, L. I. Golbe, T. Revesz, J. Hardy, A. J. Lees, B. Devlin, H. Hakonarson, U. Muller, and G. D. Schellenberg. 2011. 'Identification of common variants influencing risk of the tauopathy progressive supranuclear palsy', *Nat Genet*, 43: 699-705.

Hoozemans, J. J., E. S. van Haastert, D. A. Nijholt, A. J. Rozemuller, P. Eikelenboom, and W. Scheper. 2009. 'The unfolded protein response is activated in pretangle neurons in Alzheimer's disease hippocampus', *Am J Pathol*, 174: 1241-51.

Jicha, G. A., R. Bowser, I. G. Kazam, and P. Davies. 1997. 'Alz-50 and MC-1, a new monoclonal antibody raised to paired helical filaments, recognize conformational epitopes on recombinant tau', *J Neurosci Res*, 48: 128-32.

Johnson, G. V. W., and W. H. Stoothoff. 2004. 'Tau phosphorylation in neuronal cell function and dysfunction', *Journal of Cell Science*, 117: 5721-29.

Julier, C., and M. Nicolino. 2010. 'Wolcott-Rallison syndrome', *Orphanet J Rare Dis*, 5: 29.

Kanemaru, K., K. Takio, R. Miura, K. Titani, and Y. Ihara. 1992. 'Fetal-type phosphorylation of the tau in paired helical filaments', *J Neurochem*, 58: 1667-75.

Kansanen, E., S. M. Kuosmanen, H. Leinonen, and A. L. Levonen. 2013. 'The Keap1-Nrf2 pathway: Mechanisms of activation and dysregulation in cancer', *Redox Biol*, 1: 45-9.

Lannuzel, A., G. U. Hoglinger, S. Verhaeghe, L. Gire, S. Belson, M. Escobar-Khondiker, P. Poullain, W. H. Oertel, E. C. Hirsch, B. Dubois, and M. Ruberg. 2007. 'Atypical parkinsonism in Guadeloupe: a common risk factor for two closely related phenotypes?', *Brain*, 130: 816-27.

Lannuzel, A., P. P. Michel, G. U. Hoglinger, P. Champy, A. Jousset, F. Medja, A. Lombes, F. Darios, C. Gleye, A. Laurens, R. Hocquemiller, E. C. Hirsch, and M. Ruberg. 2003. 'The mitochondrial complex I inhibitor annonacin is toxic to mesencephalic dopaminergic neurons by impairment of energy metabolism', *Neuroscience*, 121: 287-96.

Lee, V. M. Y., M. Goedert, and J. Q. Trojanowski. 2001. 'Neurodegenerative tauopathies', *Annual Review of Neuroscience*, 24: 1121-59.

Litvan, I., Y. Agid, D. Calne, G. Campbell, B. Dubois, R. C. Duvoisin, C. G. Goetz, L. I. Golbe, J. Grafman, J. H. Growdon, M. Hallett, J. Jankovic, N. P. Quinn, E. Tolosa, and D. S. Zee. 1996. 'Clinical research criteria for the diagnosis of progressive supranuclear palsy (Steele-Richardson-Olszewski syndrome): report of the NINDS-SPSP international workshop', *Neurology*, 47: 1-9.

Litvan, I., and M. Hutton. 1998. 'Clinical and genetic aspects of progressive supranuclear palsy', *J Geriatr Psychiatry Neurol*, 11: 107-14.

Litvan, I., C. A. Mangone, A. McKee, M. Verny, A. Parsa, K. Jellinger, L. D'Olhaberriague, K. R. Chaudhuri, and R. K. Pearce. 1996. 'Natural history of progressive supranuclear palsy (Steele-Richardson-Olszewski syndrome) and clinical predictors of survival: a clinicopathological study', *J Neurol Neurosurg Psychiatry*, 60: 615-20.

Liu, F., and C. X. Gong. 2008. 'Tau exon 10 alternative splicing and tauopathies', *Mol Neurodegener*, 3: 8.

Lotharius, J., J. Falsig, J. van Beek, S. Payne, R. Dringen, P. Brundin, and M. Leist. 2005. 'Progressive degeneration of human mesencephalic neuron-derived cells triggered by dopamine-dependent oxidative stress is dependent on the mixed-lineage kinase pathway', *J Neurosci*, 25: 6329-42.

Mandell, J. W., and G. A. Banker. 1996. 'A spatial gradient of tau protein phosphorylation in nascent axons', *J Neurosci*, 16: 5727-40.

Matsumoto, H., S. Miyazaki, S. Matsuyama, M. Takeda, M. Kawano, H. Nakagawa, K. Nishimura, and S. Matsuo. 2013. 'Selection of autophagy or apoptosis in cells exposed to ER-stress depends on ATF4 expression pattern with or without CHOP expression', *Biol Open*, 2: 1084-90.

Melquist, S., D. W. Craig, M. J. Huentelman, R. Crook, J. V. Pearson, M. Baker, V. L. Zismann, J. Gass, J. Adamson, S. Szelinger, J. Corneveaux, A. Cannon, K. D. Coon, S. Lincoln, C. Adler, P. Tuite, D. B. Calne, E. H. Bigio, R. J. Uitti, Z. K. Wszolek, L. I. Golbe, R. J. Caselli, N. Graff-Radford, I. Litvan, M. J. Farrer, D. W. Dickson, M. Hutton, and D. A. Stephan. 2007. 'Identification of a novel risk locus for progressive supranuclear palsy by a pooled genomewide scan of 500,288 single-nucleotide polymorphisms', *Am J Hum Genet*, 80: 769-78.

Nath, U., Y. Ben-Shlomo, R. G. Thomson, H. R. Morris, N. W. Wood, A. J. Lees, and D. J. Burn. 2001. 'The prevalence of progressive supranuclear palsy (Steele-Richardson-Olszewski syndrome) in the UK', *Brain*, 124: 1438-49.

Nath, U., R. Thomson, R. Wood, Y. Ben-Shlomo, A. Lees, C. Rooney, and D. Burn. 2005. 'Population based mortality and quality of death certification in progressive supranuclear palsy (Steele-Richardson-Olszewski syndrome)', *J Neurol Neurosurg Psychiatry*, 76: 498-502.

Nijholt, D. A., A. Nolle, E. S. van Haastert, H. Edelijn, R. F. Toonen, J. J. Hoozemans, and W. Scheper. 2013. 'Unfolded protein response activates glycogen synthase kinase-3 via selective lysosomal degradation', *Neurobiol Aging*, 34: 1759-71.

Nijholt, D. A., E. S. van Haastert, A. J. Rozemuller, W. Scheper, and J. J. Hoozemans. 2012. 'The unfolded protein response is associated with early tau pathology in the hippocampus of tauopathies', *J Pathol*, 226: 693-702.

Pastor, P., M. Ezquerra, E. Tolosa, E. Munoz, M. J. Marti, F. Valldeoriola, J. L. Molinuevo, M. Calopa, and R. Oliva. 2002. 'Further extension of the H1 haplotype associated with progressive supranuclear palsy', *Mov Disord*, 17: 550-6.

Pilch, B., E. Allemand, M. Facompre, C. Bailly, J. F. Riou, J. Soret, and J. Tazi. 2001. 'Specific inhibition of serine- and arginine-rich splicing factors phosphorylation, spliceosome assembly, and splicing by the antitumor drug NB-506', *Cancer Res*, 61: 6876-84.

Radford, H., J. A. Moreno, N. Verity, M. Halliday, and G. R. Mallucci. 2015. 'PERK inhibition prevents tau-mediated neurodegeneration in a mouse model of frontotemporal dementia', *Acta Neuropathol*, 130: 633-42.

Rajput, A., and A. H. Rajput. 2001. 'Progressive supranuclear palsy: clinical features, pathophysiology and management', *Drugs Aging*, 18: 913-25.

Rehman, H. U. 2000. 'Progressive supranuclear palsy', *Postgrad Med J*, 76: 333-6.

Respondek, G., S. Roeber, H. Kretzschmar, C. Troakes, S. Al-Sarraj, E. Gelpi, C. Gaig, W. Z. Chiu, J. C. van Swieten, W. H. Oertel, and G. U. Hoglinger. 2013. 'Accuracy of the National Institute for Neurological Disorders and Stroke/Society for Progressive Supranuclear Palsy and neuroprotection and natural history in Parkinson plus syndromes criteria for the diagnosis of progressive supranuclear palsy', *Mov Disord*, 28: 504-9.

Run, X., Z. Liang, L. Zhang, K. Iqbal, I. Grundke-Iqbal, and C. X. Gong. 2009. 'Anesthesia induces phosphorylation of tau', *J Alzheimers Dis*, 16: 619-26.

Santiago, J. A., and J. A. Potashkin. 2014. 'A network approach to diagnostic biomarkers in progressive supranuclear palsy', *Mov Disord*, 29: 550-5.

Santpere, G., B. Puig, and I. Ferrer. 2006. 'Low molecular weight species of tau in Alzheimer's disease are dependent on tau phosphorylation sites but not on delayed post-mortem delay in tissue processing', *Neurosci Lett*, 399: 106-10.

Scheper, W., and J. J. Hoozemans. 2013. 'A new PERKspective on neurodegeneration', *Sci Transl Med*, 5: 206fs37.

Schneider, A., J. Biernat, M. von Bergen, E. Mandelkow, and E. M. Mandelkow. 1999. 'Phosphorylation that detaches tau protein from microtubules (Ser262, Ser214) also protects it against aggregation into Alzheimer paired helical filaments', *Biochemistry*, 38: 3549-58.

Scholz, D., D. Poltl, A. Genewsky, M. Weng, T. Waldmann, S. Schildknecht, and M. Leist. 2011. 'Rapid, complete and large-scale generation of post-mitotic neurons from the human LUHMES cell line', *J Neurochem*, 119: 957-71.

Silver, I. A., and M. Erecinska. 1994. 'Extracellular glucose concentration in mammalian brain: continuous monitoring of changes during increased neuronal activity and upon limitation in oxygen supply in normo-, hypo-, and hyperglycemic animals', *J Neurosci*, 14: 5068-76.

Sou, S. N., K. M. Ilieva, and K. M. Polizzi. 2012. 'Binding of human BiP to the ER stress transducers IRE1 and PERK requires ATP', *Biochem Biophys Res Commun*, 420: 473-8.

Spillantini, M. G., J. R. Murrell, M. Goedert, M. R. Farlow, A. Klug, and B. Ghetti. 1998. 'Mutation in the tau gene in familial multiple system tauopathy with presenile dementia', *Proc Natl Acad Sci U S A*, 95: 7737-41.

Stamelou, M., R. de Silva, O. Arias-Carrion, E. Boura, M. Hollerhage, W. H. Oertel, U. Muller, and G. U. Hoglinger. 2010. 'Rational therapeutic approaches to progressive supranuclear palsy', *Brain*, 133: 1578-90.

Steele, J. C., J. C. Richardson, and J. Olszewski. 1964. 'Progressive Supranuclear Palsy. A Heterogeneous Degeneration Involving the Brain Stem, Basal Ganglia and Cerebellum with Vertical Gaze and Pseudobulbar Palsy, Nuchal Dystonia and Dementia', *Arch Neurol*, 10: 333-59.

Stutzbach, L. D., S. X. Xie, A. C. Naj, R. Albin, S. Gilman, P. S. P. Genetics Study Group, V. M. Lee, J. Q. Trojanowski, B. Devlin, and G. D. Schellenberg. 2013. 'The unfolded protein response is activated in disease-affected brain regions in progressive supranuclear palsy and Alzheimer's disease', *Acta Neuropathol Commun*, 1: 31.

Trinh, M. A., H. Kaphzan, R. C. Wek, P. Pierre, D. R. Cavener, and E. Klann. 2012. 'Brain-specific disruption of the eIF2alpha kinase PERK decreases ATF4 expression and impairs behavioral flexibility', *Cell Rep*, 1: 676-88.

Verny, M., C. Duyckaerts, Y. Agid, and J. J. Hauw. 1996. 'The significance of cortical pathology in progressive supranuclear palsy. Clinico-pathological data in 10 cases', *Brain*, 119 (Pt 4): 1123-36.

Vidal, R. L., and C. Hetz. 2012. 'Crosstalk between the UPR and autophagy pathway contributes to handling cellular stress in neurodegenerative disease', *Autophagy*, 8: 970-2.

Wade-Martins, R. 2012. 'Genetics: The MAPT locus-a genetic paradigm in disease susceptibility', *Nat Rev Neurol*, 8: 477-8.

Warren, N. M., and D. J. Burn. 2007. 'Progressive supranuclear palsy', *Pract Neurol*, 7: 16-23.

Weingarten, M. D., A. H. Lockwood, S. Y. Hwo, and M. W. Kirschner. 1975. 'A protein factor essential for microtubule assembly', *Proc Natl Acad Sci U S A*, 72: 1858-62.

Wiersma, V. I., W. van Hecke, W. Scheper, M. A. van Osch, W. J. Hermsen, A. J. Rozemuller, and J. J. Hoozemans. 2016. 'Activation of the unfolded protein response and granulovacuolar degeneration are not common features of human prion pathology', *Acta Neuropathol Commun*, 4: 113.

Will, C. L., and R. Luhrmann. 2011. 'Spliceosome structure and function', *Cold Spring Harb Perspect Biol*, 3.

Williams, D. R., and A. J. Lees. 2009. 'Progressive supranuclear palsy: clinicopathological concepts and diagnostic challenges', *Lancet Neurol*, 8: 270-9.

Xu, C., B. Bailly-Maitre, and J. C. Reed. 2005. 'Endoplasmic reticulum stress: cell life and death decisions', *J Clin Invest*, 115: 2656-64.

Xu, H., T. W. Rosler, T. Carlsson, A. de Andrade, J. Bruch, M. Hollerhage, W. H. Oertel, and G. U. Hoglinger. 2014. 'Memory Deficits Correlate with Tau and Spine Pathology in P301S MAPT Transgenic Mice', *Neuropathol Appl Neurobiol*.

Yamada, E. S., G. Respondek, S. Mussner, A. de Andrade, M. Hollerhage, C. Depienne, A. Rastetter, A. Tarze, B. Friguet, M. Salama, P. Champy, W. H. Oertel, and G. U. Hoglinger. 2014. 'Annonacin, a natural lipophilic mitochondrial complex I inhibitor, increases phosphorylation of tau in the brain of FTDP-17 transgenic mice', *Exp Neurol*, 253C: 113-25.

Zhang, P., B. McGrath, S. Li, A. Frank, F. Zambito, J. Reinert, M. Gannon, K. Ma, K. McNaughton, and D. R. Cavener. 2002. 'The PERK eukaryotic initiation factor 2 alpha kinase is required for the development of the skeletal system, postnatal growth, and the function and viability of the pancreas', *Mol Cell Biol*, 22: 3864-74.

Zhong, X. Y., J. H. Ding, J. A. Adams, G. Ghosh, and X. D. Fu. 2009. 'Regulation of SR protein phosphorylation and alternative splicing by modulating kinetic interactions of SRPK1 with molecular chaperones', *Genes Dev*, 23: 482-95.

Zhou, J., Q. Yu, and T. Zou. 2008. 'Alternative splicing of exon 10 in the tau gene as a target for treatment of tauopathies', *BMC Neurosci*, 9 Suppl 2: S10.

Acknowledgements

First and foremost, I would like to express my sincere gratitude to my advisor Prof. Dr. Günter Höglinger for the continuous support of my doctoral study and research, for his patience, motivation, enthusiasm and experience. His guidance helped me at all times throughout the research. I could not have imagined having a better advisor and mentor.

My sincere thanks also go to Prof. Dr. Stefan Lichtenthaler (Technische Universität München) and Prof. Dr. Konstanze Winklhofer (Ruhr-Universität Bochum) as further advisors. They spent many hours discussing the research project and providing extremely valuable advice and encouragement.

I would also like to extend my gratitude to Prof. Dr. Michel Goedert of the University of Cambridge. He served as an additional advisor and took many hours of his valuable time every time I saw him to discuss my research. He substantially helped and advised me in questions regarding different ways to detect tau pathology.

I am extremely grateful to the Bavarian Research Foundation (Bayerische Forschungsstiftung) for funding me for the purpose of my doctoral studies. They have been very generous in not only supporting me but also providing funds for travel. The research would not have been possible without them.

The research project also critically depended on funds provided via Prof. Günter Höglinger from the Deutsche Forschungsgemeinschaft (DFG, HO2402/6-1) and the German Centre for Neurodegenerative Diseases (DZNE e.V.). DZNE also provided laboratory space and essential equipment.

I would also like to thank Prof. Mel Feany of Harvard Medical School, Boston, USA, for allowing me to spend time in her laboratory and teaching me valuable research tools in genetics.

Many others provided very helpful advice and materials necessary for the project. Dr Thomas Arzberger and the Netherlands Brain Bank generously provided samples of human PSP and control brain tissue. Dr Pierre Champy, CNRS UMR 8076 BioCIS, Univ. Paris–Sud, Châtenay-Malabry, France, extracted the annonacin. Cécile Julier and Valérie Senée performed the PERK mutation analysis for the WRS case.

I am also very grateful to Hong Xu, Anderson de Andrade and Robin Konhäuser for introducing me to the techniques of the laboratory. Carolin Nierwetberg, Robin Konhäuser, Magda Baba and Brigitte Kraft provided valuable technical assistance.

Last but not least I would like to thank all my laboratory colleagues for their stimulating discussions and mutual support: Johannes Melms, Thomas Koegelsperger, Matthias Höllerhage, Thomas Rösler, Sigrid Schwarz, Carolin Kurz, Natascha Fussi, Tasnim Chakroun, Yvonne Roedenbeck, Kerstin Schweyer, Elizabeth Findeiss, Gesine Respondek, Sylvia Maaß.

Ultimately, I would like to thank my parents Janni Bruch and Mathias Bruch for their love and support throughout the time of the project.

Enclosed publications

Publication 1: Mitochondrial Complex 1 Inhibition Increases 4-Repeat Isoform Tau by SRSF2 Upregulation

Full reference:
Bruch J, Xu H, De Andrade A, & Hoglinger G (2014) Mitochondrial Complex 1 Inhibition Increases 4-Repeat Isoform Tau by SRSF2 Upregulation. PloS one 9(11):e113070

Permission to reprint:

The following policy applies to all of PLOS journals, unless otherwise noted.

PLOS applies the Creative Commons Attribution (CC BY) license to works we publish. This license was developed to facilitate open access – namely, free immediate access to, and unrestricted reuse of, original works of all types.

Under this license, authors agree to make articles legally available for reuse, without permission or fees, for virtually any purpose. Anyone may copy, distribute or reuse these articles, as long as the author and original source are properly cited.

Publication 2: Early Neurodegeneration in the Brain of a Child Without Functional PKR-like Endoplasmic Reticulum Kinase

Full reference:
Bruch J, et al. (2015) Early Neurodegeneration in the Brain of a Child Without Functional PKR-like Endoplasmic Reticulum Kinase. J Neuropathol Exp Neurol 74(8):850-857

Permission to reprint:

Copyright Clearance Center RightsLink®

Home | Create Account | Help | Live Chat

Wolters Kluwer

Title: Early Neurodegeneration in the Brain of a Child Without Functional PKR-like Endoplasmic Reticulum Kinase

Author: Julius Bruch, Carolin Kurz, Alexandre Vasiljevic, et al

Publication: Journal of Neuropathology and Experimental Neurology

Publisher: Wolters Kluwer Health, Inc.

Date: Jan 1, 2015

Copyright © 2015, (C) 2015 by American Association of Neuropathologists, Inc.

LOGIN

If you're a copyright.com user, you can login to RightsLink using your copyright.com credentials. Already **a RightsLink user** or want to learn more?

This reuse is free of charge. No permission letter is needed from Wolters Kluwer Health, Lippincott Williams & Wilkins. We require that all authors always include a full acknowledgement. Example: AIDS: 13 November 2013 - Volume 27 - Issue 17 - p 2679-2689. Wolters Kluwer Health Lippincott Williams & Wilkins© No modifications will be permitted.

BACK | CLOSE WINDOW

OPEN ACCESS Freely available online

PLOS ONE

Mitochondrial Complex 1 Inhibition Increases 4-Repeat Isoform Tau by SRSF2 Upregulation

Julius Bruch[1,2☯], Hong Xu[1,2☯], Anderson De Andrade[1], Günter Höglinger[1,2]*

1 Department of Translational Neurodegeneration, German Centre for Neurodegenerative Diseases (DZNE), Munich, Germany, **2** Department of Neurology, Technische Universität München, Munich, Germany

Abstract

Progressive Supranuclear Palsy (PSP) is a neurodegenerative disorder characterised by intracellular aggregation of the microtubule-associated protein tau. The tau protein exists in 6 predominant isoforms. Depending on alternative splicing of exon 10, three of these isoforms have four microtubule-binding repeat domains (4R), whilst the others only have three (3R). In PSP there is an excess of the 4R tau isoforms, which are thought to contribute significantly to the pathological process. The cause of this 4R increase is so far unknown. Several lines of evidence link mitochondrial complex I inhibition to the pathogenesis of PSP. We demonstrate here for the first time that annonacin and MPP^+, two prototypical mitochondrial complex I inhibitors, increase the 4R isoforms of tau in human neurons. We show that the splicing factor SRSF2 is necessary to increase 4R tau with complex I inhibition. We also found SRSF2, as well as another tau splicing factor, TRA2B, to be increased in brains of PSP patients. Thereby, we provide new evidence that mitochondrial complex I inhibition may contribute as an upstream event to the pathogenesis of PSP and suggest that splicing factors may represent an attractive therapeutic target to intervene in the disease process.

Citation: Bruch J, Xu H, De Andrade A, Höglinger G (2014) Mitochondrial Complex 1 Inhibition Increases 4-Repeat Isoform Tau by SRSF2 Upregulation. PLoS ONE 9(11): e113070. doi:10.1371/journal.pone.0113070

Editor: Oscar Arias-Carrion, Hospital General Dr. Manuel Gea González, Mexico

Received July 11, 2014; **Accepted** October 23, 2014; **Published** November 17, 2014

Data Availability: The authors confirm that all data underlying the findings are fully available without restriction. All relevant data are within the paper.

Funding: J.B. was funded by the Bavarian Research Foundation (Bayerische Forschungsstiftung), H.X. by the DAAD (German Academic Exchange Service), G.U.H. by the DFG (Deutsche Forschungsgemeinschaft, HO2402/6-2). The funders had no role in study design, data collection and analysis, decision to publish, or preparation of the manuscript.

Competing Interests: The authors have declared that no competing interests exist.

* Email: hoeglinger@lrz.tum.de

☯ These authors contributed equally to this work.

Introduction

Tauopathies are a heterogeneous group of neurodegenerative diseases with the common feature of intracellular aggregation of the microtubule associated protein tau. They include, but are not limited to, Alzheimer's Disease, Progressive Supranuclear Palsy (PSP), Argyrophilic Grain Disease (AGD), Corticobasal Degeneration (CBD), Pick's Disease and some other forms of frontotemporal dementias. Different tauopathies vary significantly in their clinical and pathological phenotype [1].

In the human central nervous system there are six predominant splicing variants of the *MAPT* gene, encoding tau proteins. These depend on the exclusion or inclusion of exons 2, 3 and 10: 3R0N, 3R1N, 3R2N, 4R0N, 4R1N and 4R2N [2]. 0N signifies the inclusion of neither exon 2 or 3. 1N denotes the inclusion of exon 2 but not 3, whilst 2N denotes the inclusion of both exons 2 and 3. 3R denotes the absence of exon 10, 4R its presence. Exon 10 codes for an additional microtubule binding repeat, so that 4R isoforms have 4 binding repeats, whilst 3R isoforms have only 3.

Across different tauopathies the isoform constitution varies. A common classification of tauopathies, therefore, is between the 3R isoform and the 4R isoform tauopathies [3]. While in healthy adults and in Alzheimer's disease 3R and 4R isoforms are generally in balance, PSP, CBD and AGD feature a relative excess of 4R isoforms [4]. Pick's Disease, conversely, has a relative excess of 3R isoforms. This imbalance is thought to play a major role in the pathogenesis of these tauopathies [5]. 4R isoforms are more prone to aggregation than 3R isoforms [5]. A single mutation in the *MAPT* gene affecting the inclusion of exon 10 to favour generation of 4R tau appears to be sufficient to trigger a tauopathy [6]. This has led to the hypothesis that an excess of 4R tau may be significantly pathogenic. Therefore, reducing the relative amount of 4R may be a strategy for therapy in 4R tauopathies [5,7].

Alternative splicing of exon 10 is regulated by a combination of *cis*-elements in exon 10 and intron 10, as well as by *trans*-acting factors [2]. It is through these *trans*-acting factors that alternative splicing can be modified and regulated by the cell. They are divided into heterogeneous nuclear ribonucleoproteins (hnRNPs) and serine/arginine-rich (SR) proteins or SR-like proteins. The SR proteins participate in the spliceosome and are thus involved in both constitutive splicing and the regulation of alternative splicing [8]. They are controlled through phosphorylation and acetylation and have been discussed as a potential drug target in the context of cancer treatment [9,10]. However, so far, the molecular mechanisms leading to preferential generation of 4R tau by alternative splicing of wild-type tau in sporadic 4R tauopathies are not understood.

There are several lines of evidence suggesting a role for dysfunction of the mitochondrial respiratory chain, particularly

of mitochondrial complex I, in the pathogenesis of PSP. A study using transmitochondrial cytoplasmic hybrid (cybrid) cell lines expressing mitochondrial genes from persons with PSP found complex I activity to be reduced [11]. Dysfunctional complex I is a major emitter of reactive oxygen species [12] and evidence of oxidative stress has been found in autopsy material of PSP patients [13,14]. A study using combined phosphorus and proton magnetic resonance spectroscopy has identified evidence for cerebral depletion in high-energy phosphates and increased lactate levels in PSP, a pattern compatible with a primary failure of the mitochondrial respiratory chain [15]. Finally, there is also an epidemiological association between the consumption of soursop fruit containing the mitochondrial complex I inhibitor annonacin [16] and a PSP-like tauopathy on the island of Guadeloupe [17]. Annonacin has been shown to induce a tauopathy *in vitro* in cultured neurons [16,18], as well as *in vivo* [19]. So far described are four effects of annonacin that are typical features for tauopathies, namely increased tau protein levels, tau hyperphosphorylation, redistribution of tau from the axons to the somatodendritic compartment, and eventual cell death [18]. Here, we explore the effect of complex I inhibition on the alternative splicing of tau.

Materials and Methods

Cell Culture

Nunc Nunclon Delta 6-well (for protein and mRNA) or 48-well (for cell assays) plates (Thermo Fisher Scientific, Waltham, MA, USA) were coated with 100 μg/ml poly-L-lysine (Sigma-Aldrich, St. Louis, MO, USA) and 5 μg/ml fibronectin (Sigma-Aldrich). LUHMES (Lund Human Mesencephalic) cells, derived from female human embryonic ventral mesencephalic cells by conditional immortalization [20] (Tet-off v-myc over-expression) were seeded in a concentration of 130,000 cells/cm^2 to achieve a confluence of 50%. They were then differentiated for 8 days in a medium of DMEM/F12 (Sigma-Aldrich), 1 μg/ml Tetracycline, 2 mg/ml GDNF and 490 μg/ml dbcAMP into post-mitotic neurons [21] with a dopaminergic phenotype [20]. On day 8 post differentiation the cells were treated with 25 nM annonacin, 20 μM 6-OHDA or 10 μM MPP^+ for 48 h. For the intoxication period the medium was replaced with new medium containing glucose levels reduced to 250 μM, i.e. the physiological concentration in the human brain [22]. For the starving condition, cells were incubated for 24 hours in pure DMEM (Life Technologies, Grand Island, NY, USA) with no additives and no glucose.

Human Brain Tissue and Ethics Statement

Human fresh frozen brain sections of the *locus coeruleus* area were obtained from The Netherlands Brain Bank, Netherlands Institute for Neuroscience, Amsterdam (www.brainbank.nl). All Material has been collected from donors for or from whom written informed consent for a brain autopsy and the use of the material and clinical information for research purposes had been obtained by The Netherlands Brain Bank in accordance with the Declaration of Helsinki.

Quantitative Real-Time PCR

RNA from human tissue samples was extracted by grinding the tissue in liquid nitrogen to a powder and then dissolving it in the RA1 buffer supplied as part of the NucleoSpin RNA (Macherey Nagel, Düren, Germany) RNA extraction kit +1% (v/v) 2-Mercaptoethanol (Sigma-Aldrich). RNA from cells was extracted by scraping the cells from the culture plate with RA1 buffer +1% (v/v) 2-Mercaptoethanol. The remaining extraction procedure was according to the manufacturer's instructions for the NucleoSpin RNA kit. RNA concentrations were determined using the NanoDrop 2000c Spectrophotometer (Thermo Fisher Scientific). The RNA was then transcribed into cDNA with the iScript cDNA Synthesis Kit (BioRad, Berkeley, CA, USA) using the manufacturer's instructions. Real-Time PCR was performed on the Applied Biosystems StepOnePlus (Life Technologies) system using TaqMan Universal Master Mix II and TaqMan primers against total *MAPT, MAPT 0N, MAPT 1N, MAPT 2N, MAPT 3R, MAPT 4R, SRSF1, SRSF2, SRSF3, SRSF6, SRSF7, SRSF9, SRSF11* and *TRA2B*. *PSMC1* and *POL2A* were used as reference genes for relative quantification in all tau splicing factor experiments, while *PPIB* and *GAPDH* were used in all tau isoform experiments as they were determined to be the most stably expressed across the respective experimental conditions. All values are relative quantities compared to untreated (control) cells. Three biological repeats with three technical repeats each were analysed. Analysis was conducted with the Applied Biosystems StepOnePlus (Life Technologies) and Qbase+ (Biogazelle, Zwijnaarde, Belgium) software packages. Absolute quantification was performed by creating a standard curve with plasmids containing either the 2N3R or the 2N4R spliced variant of *MAPT* (obtained as a gift from Eva-Maria Mandelkow, DZNE Bonn, Germany). The absolute quantity was computed by deriving the relationship between CT values and absolute quantity with the StepOne Plus software.

Western Blotting

Protein was extracted from cells using the M-PER Mammalian Protein Extraction Reagent (Thermo Fisher Scientific). The protein solution was frozen at −80°C immediately after retrieval and for a minimum of two hours. The solution was then thawed on ice, vortexed, centrifuged at 5000 g for 15 minutes at 4°C and the supernatant retrieved. Total protein concentrations were determined using the BCA kit (Thermo Fisher Scientific) by heating the samples at 60°C for 30 minutes and measuring the absorption on the NanoDrop 2000c Spectrophotometer (Thermo Fisher Scientific). 20 μg of total protein were then adjusted to equal concentrations between samples by dilution with M-PER and subsequently heated at 95°C for 5 minutes with 1× Roti-Load loading buffer (Carl Roth, Karlsruhe, Germany). SDS-PAGE was performed using precast Gels (anyKD, Bio-Rad) in a tris-glycine running buffer (14.4% glycine, 3% Tris, 1% SDS w/v, Carl Roth). The protein was blotted onto PVDF membrane (Bio-Rad) at 70 V for 65 minutes. The membrane was blocked with 1× Roti-Block solution (Carl Roth) for 1h and then incubated at 4°C overnight under gentle shaking with the primary antibody (table 1) in TBS with 5% BSA (Cell Signaling, Danvers, MA, USA) and 0.05% TWEEN (Sigma-Aldrich). The membranes were then washed and incubated with the appropriate secondary antibody at 1:2500 (v/v) in 1× Roti-Block solution for 2 h, followed by further washing and exposure to Clarity Western ECL Substrate (Bio-Rad) or, in the case of 4-repeat tau, to **ECL solution** (General Electric, Fairfield, CT, USA). Chemiluminescence was detected with the Gel image System (Bio-Rad) and analysed by background subtracted optical density analysis with ImageLab software (Bio-Rad).

siRNA Silencing

LUHMES cells were seeded out and differentiated as described above and allowed to adhere to the plate floor for 4 h. siRNA (Sigma-Aldrich) targeted against SRSF2 (final concentration 200 nM) and Lipofectamine RNAiMAX (Life Technologies) (final concentration 1.2 μl/ml) were dissolved in separate aliquots of

Table 1. Primary Antibody Concentrations Used.

Antigen	Clone	Species	Concentration (v/v)	Company
Human tau	HT7	Mouse	1:1000	Pierce Antibodies, Thermo
3-repeat tau	8E6/C11	Mouse	1:500	Millipore
4-repeat tau	1E1/A6	Mouse	1:300	Millipore
Actin (I-19)	Polyclonal	Goat	1:2500	Santa Cruz Biotechnologies

doi:10.1371/journal.pone.0113070.t001

medium (OptiMEM, Life Technologies). The diluted siRNA was then added to the diluted Lipofectamine RNAiMAX. The combined solution was then allowed to incubate for 20 minutes before being added to the cells.

ATP Assay

ATP assays were conducted using the ATP test kit by Lonza according to the manufacturer's instructions. Luminescence was read with the FLUOstar Omega platereader (BMG Labtech). The data was analysed using the MARS Data Analysis Software (BMG Labtech).

MTT Assay

Thiazolyl Blue Tetrazolium Blue (MTT) (Sigma Aldrich) was dissolved in sterile PBS to a concentration of 5 mg/ml. This stock solution was added to the cells in culture medium to achieve a final concentration of 0.5 mg/ml. The 48-well culture plate was then incubated at 37°C for 1 h, the medium removed completely and frozen at −80°C for 1 h. The plate was then thawed, 300 µl DMSO (AppliChem, Darmstadt, Germany) was added per well and the plate was shaken to ensure complete dissolution of the violet crystals. 100 µl from each well were transferred to a new 96-well plate and the absorbance was read with the platereader at a wavelength of 590 nm (reference wave length 630 nm). The data was analysed using the MARS Data Analysis Software (BMG Labtech).

Statistics

Prism 6 (GraphPad Software, La Jolla, CA, USA) was used for statistical calculations and for the creation of line and bar graphs. Results were compared by 2-way ANOVA with Sidak post-hoc test, unless stated otherwise. Data are shown as mean ± SEM. $P < 0.05$ was considered significant.

Results

Annonacin Causes an Upregulation of the Tau 4-Repeat Isoform

We first characterized expression of tau isoforms in LUHMES cells, a cell culture line of human mesencephalic neurons, derived from female human embryonic ventral mesencephalic cells by conditional immortalization (Tet-off v-myc over-expression) [21]. These cells start expressing the 4-repeat (4R) isoform of tau from day 8 post differentiation into a neuronal phenotype. On day 10, 4R-spliced mRNA makes up 3.9% ±0.3 (n = 3) of the total MAPT mRNA. We used this human neuronal model for the present work as rodent cells express only 4R tau.

When treated with annonacin at a concentration of 25 nM for 48 h from days 8 to 10 post differentiation, LUHMES cells remain 60.7±0.4% viable (MTT assay) with an ATP concentration of 64±1% compared to that of untreated cells (figure 1A).

Under these conditions we observed the mRNA of the 4R isoforms of tau to be upregulated significantly (figure 1B) compared with untreated cells, as determined by quantitative PCR. There was no significant change in the relative quantity of 3R isoforms. The level of inclusion of exons 2 and 3 also did not change significantly, although there was a slight increase in the amount of 0N isoforms. This indicates that annonacin selectively increases inclusion of exon 10 with no or little relative effect on the alternative splicing of the other exons.

We also observed an upregulation of the 4R tau isoforms on the protein level by Western blot (figure 1C). 3R tau was again not significantly changed. The level of upregulation at the protein level is very similar to that on the mRNA level, suggesting a tight correlation between the regulation of alternative splicing and the isoform distribution seen at the protein level. There was no significant increase in the amount of total tau with annonacin, probably due to the greater proportion of 3R isoforms in LUHMES cells of this age.

The Splicing Factor SRSF2 Is Necessary for Annonacin-Mediated Alternative Splicing

We next explored the mechanism of how annonacin induces this isoform change. We tested 10 splicing factors known to influence the inclusion or exclusion of exon 10 in the MAPT gene [2] by quantitative PCR. An overview of the splicing factors tested is shown in table 2.

We found SRSF2 to be the only splicing factor significantly upregulated with annonacin treatment that is known to promote the inclusion of exon 10 (figure 2A). This prompted us to explore whether SRSF2 has a functional role to play in annonacin mediated 4R upregulation. We knocked down *SRSF2* with siRNA starting from 6 hours post differentiation in LUHMES cells and treated these cells with annonacin from days 8–10, as in the previous experiments. At day 10, *SRSF2* was reduced by half. In spite of this incomplete silencing efficiency, the 4R isoform of *MAPT* in annonacin treated cells was reduced dramatically compared to untreated cells (figure 2B). This suggests that SRSF2 plays a critical role in the upregulation of the 4R MAPT isoforms seen upon annonacin treatment.

More Splicing Factors Are Upregulated in Human PSP

We also tested splicing factor expression levels in human brain tissue of the *locus coeruleus* of 4 PSP patients and five control patients free of psychiatric or neurodegenerative diseases (table 3). This time, however, we limited our analysis to those splicing factors known to increase *MAPT* exon 10 inclusion. We confirmed the increase of the 4R isoform in the PSP patients compared to the controls (figure 2C). Expression of the splicing factors *SRSF2* and *TRA2B* was also increased significantly. This suggests that the increase in 4R isoforms seen with annonacin treatment may

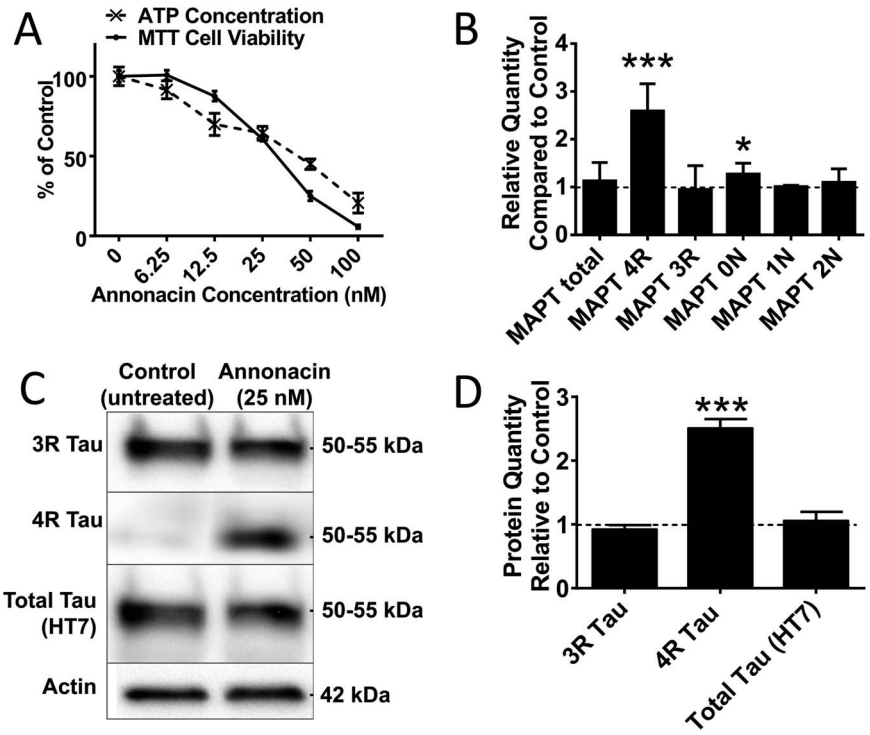

Figure 1. Annonacin Causes an Upregulation of the 4R Isoforms of Tau. A) LUHMES neurons were treated with different concentrations of annonacin for 48 h from day 8–10 post differentiation (n = 12). The MTT test, a measure for mitochondrial reducing function, and ATP concentration, are expressed as a relative percentage compared to untreated control cells. B) 4R isoform (exon 10) mRNA is upregulated with annonacin treatment. Quantitative PCR results showing the relative quantity of mRNA for different *MAPT* splicing variants in cells treated with 25 nM annonacin for 48 h from day 8–10 post differentiation compared to untreated cells (dotted line). 3 biological repeats with 3 technical repeats each. ***: $p<0.001$, *: $p<0.05$ vs. untreated cells (2-way ANOVA with Sidak's post-hoc test). C) 4R isoform protein is upregulated with annonacin treatment. Western blot for 3R and 4R isoforms of tau protein, as well as total tau (detected with the HT7 antibody). LUHMES cells were either left untreated or treated with 25 nM annonacin. Actin was used as loading control. D) Quantification of figure 1C. Results show the relative quantity (fold-change) compared to untreated control cells (relative quantity = 1, represented by dotted line). 3 biological repeats. ***: $p<0.001$ vs. untreated cells (2-way ANOVA with Sidak's post-hoc test).
doi:10.1371/journal.pone.0113070.g001

account partly for the mechanism by which 4R isoform tau is upregulated in PSP.

4R Tau Upregulation Occurs with Other Complex I Inhibitors but Not Oxidative Stress

We tested whether 4R isoform upregulation upon annonacin treatment is a non-specific consequence of neuronal injury, specific to mitochondrial complex I inhibition or even more specific to annonacin. We therefore repeated the experiment with 1-methyl-4-phenylpyridinium (MPP^+), another complex I inhibitor, 6-hydroxydopamine (6-OHDA), a neurotoxin known to be neurotoxic primarily through oxidative stress [23] and by starving the cells of glucose and nutrients. As shown in figures 3 A and B, a comparable level of toxicity and ATP reduction to

Table 2. Overview of the splicing factors known to influence MAPT exon 10 alternative splicing.

Splicing factor	Target *cis*-element	Effect on exon 10 splicing
SRSF1 (SRp30a, ASF)	PPE	Inclusion
SRSF2 (SRp30b, SC35)	SC35-like	Inclusion
SRSF3 (SRp20)	ND	Exclusion
SRSF4 (SRp75)	ND	Exclusion
SRSF6 (SRp55)	ND	Exclusion
SRSF7 (9G8)	ISS	Exclusion
SRSF9 (SRp30c)	ND	Inclusion
SRSF11 (SRp54)	PPE	Exclusion
TRA2B	PPE	Inclusion

Source: Adapted from [2].
doi:10.1371/journal.pone.0113070.t002

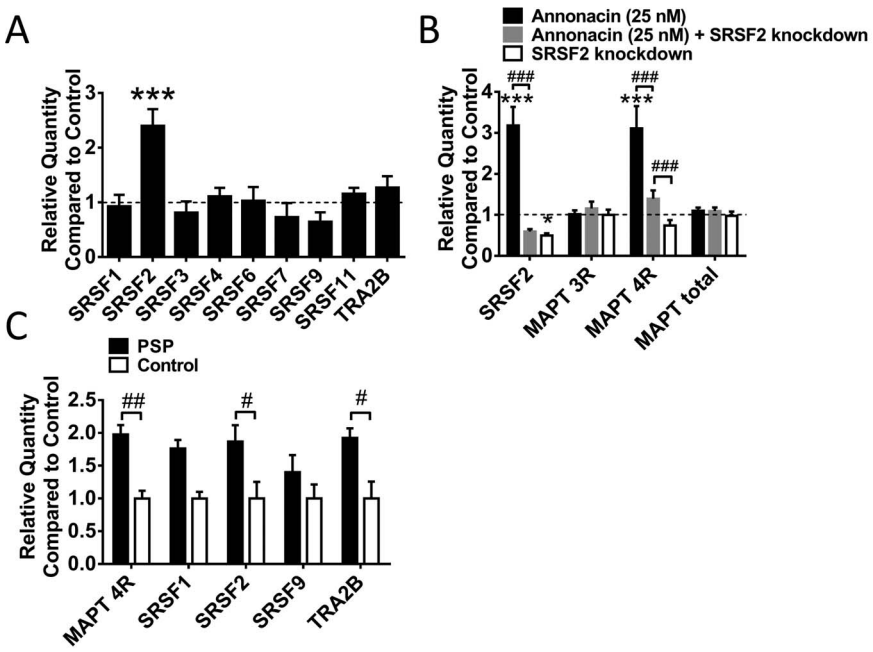

Figure 2. SRSF2 is a Critical Player in Annonacin Mediated Tau Alternative Splicing. A) Quantitative PCR results for 9 different splicing factors known to have an effect on exon 10 alternative splicing (table 2). Data shown are relative quantities compared to untreated cells (dotted line). Only SRSF2 was elevated significantly with annonacin treatment. All other splicing factors tested were not significantly elevated. 3 biological repeats with 3 technical repeats each. ***: $p<0.001$, *: $p<0.05$ vs. untreated control (2-way ANOVA with Sidak's post-hoc test). B) Quantitative PCR results for LUHMES cells on day 10 post differentiation treated with SRSF2 knockdown siRNA for 10 days and/or with annonacin for 48 h. 3 biological repeats with 3 technical repeats each. ***: $p<0.001$ vs. untreated control (dotted line); ###: $p<0.001$ (2-way ANOVA with Sidak's post-hoc test). C) Quantitative PCR results for the 4 splicing factors known to increase MAPT exon 10 inclusion in *locus coeruleus* tissue of four PSP patients and five controls without neurodegenerative diseases. 3 biological repeats with 3 technical repeats each. #: $p<0.05$, ##: $p<0.01$ (2-way ANOVA with Sidak's post-hoc test).
doi:10.1371/journal.pone.0113070.g002

that of 25 nM annonacin is achieved by 6-OHDA at a concentration of 20 μM (22% ATP reduction) and by MPP^+ at a concentration of 10 μM (37% ATP reduction). Therefore, we decided to use these concentrations to test the MAPT isoform changes with these toxins.

With MPP^+ treatment we observed a significant increase in exon 10 inclusion on the mRNA level by qPCR (figure 3C) and in the levels of 4R tau isoforms by Western blot (figure 4A, B) compared to controls, as with annonacin. With 6-OHDA treatment and with starvation we only observed a slight reduction in both 4R and 3R isoforms. In all three cases the inclusion of exons 2 and 3 did not increase (data not shown). This would suggest that complex I inhibition in general and not oxidative stress or neuronal suffering per se is responsible for the increased level of exon 10 inclusion observed with annonacin.

Finally, we explored the role of *SRSF2* in these observations. We found that MPP^+ also acts via SRSF2 upregulation and that there is no *SRSF2* upregulation with 6-OHDA treatment or starvation.

Table 3. Overview of Human Tissue Used.

Case Number	Diagnosis	Cause of Death	Age at death	Braak Stage	Sex	Postmortem delay (hours: minutes)
P1	PSP	"Natural death"	73	2C	Male	4:20
P2	PSP	Acute heart failure	70	3	Male	6:50
P3	PSP	Aspiration pneumonia	73	2	Male	6:15
P4	PSP	Urinary tract infection	70	1A	Male	5:20
C1	Non-demented control	Pancreas carcinoma	70	0	Male	7:30
C2	Non-demented control	Prostate cancer	69	0	Male	5:55
C3	Non-demented control	Lung emboli (clinical suspicion)	73	0	Male	24:45
C4	Non-demented control	Sepsis	71	1	Male	7:40
C5	Non-demented control	Myocardial infarction	67	1B	Male	18:35

doi:10.1371/journal.pone.0113070.t003

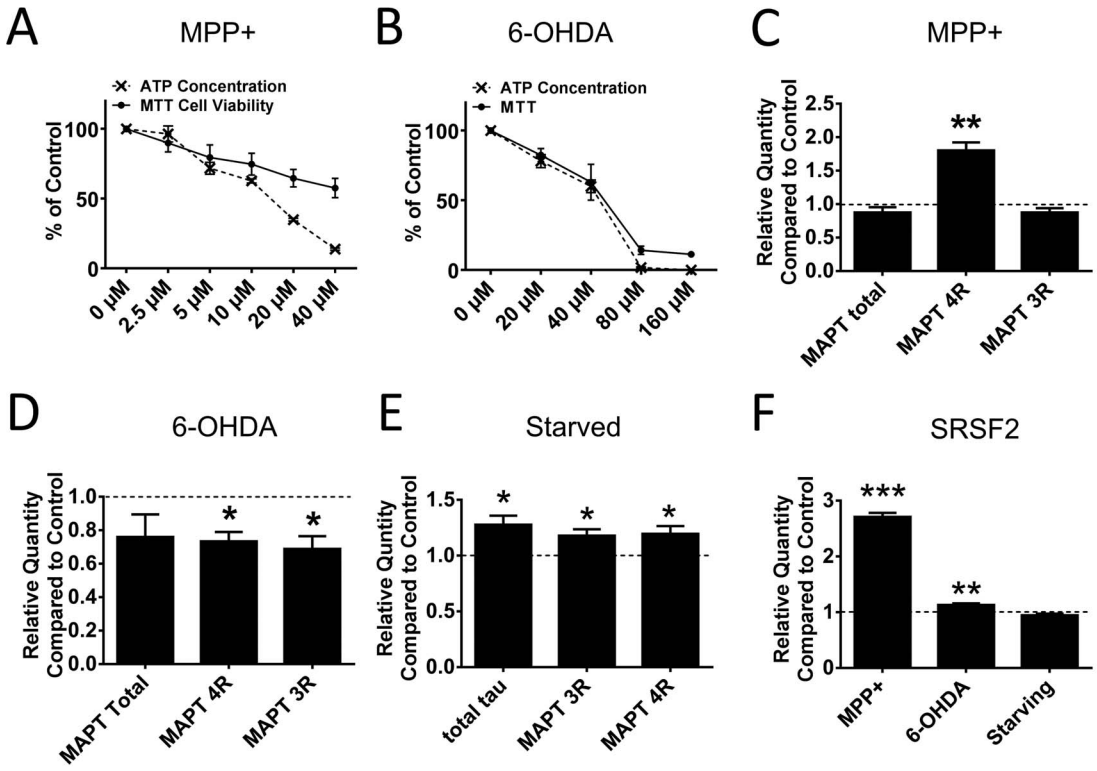

Figure 3. The 4R Isoform Shift Can Be Reproduced with Another Complex I Inhibitor but not with the Oxidative Stressor 6-OHDA. A) ATP concentration and MTT cell viability in LUHMES cells as measured by the MTT assay for different concentrations of 6-OHDA. Treatment was for 48 h from day 8–10 post differentiation. n = 12. B) ATP concentration and MTT cell viability in LUHMES cells as measured by the MTT assay for different concentrations of MPP+. Treatment was for 48 h from day 8–10 post differentiation. n = 12. C) Quantitative PCR results of MAPT splicing variants for LUHMES cells treated with 10 µM MPP^+ for 48 h from day 8–10 post differentiation. 3 biological repeats with 3 technical repeats each. **: $p<0.01$ vs. untreated cells (dotted line), (2-way ANOVA with Sidak's post-hoc test). D) Quantitative PCR results of MAPT splicing variants for LUHMES cells treated with 20 µM 6-OHDA for 48 h from day 8–10 post differentiation. 3 biological repeats with 3 technical repeats each. *: $p<0.05$ vs. untreated cells (dotted line), (2-way ANOVA with Sidak's post-hoc test). E) Quantitative PCR results of MAPT splicing variants for LUHMES cells starved of nutrients and glucose for 24 h from day 8–9 post differentiation. 3 biological repeats with 3 technical repeats each. *: $p<0.05$ vs. untreated cells (dotted line), (2-way ANOVA with Sidak's post-hoc test). F) Quantitative PCR results of SRSF2 for LUHMES cells treated with 10 µM MPP^+ or 20 µM 6-OHDA for 48 h from day 8–10 post differentiation or starved for 24 h from day 8–9 post differentiation. 3 biological repeats with 3 technical repeats each. *: $p<0.05$, **: $p<0.01$ vs. untreated cells (dotted line), (2-way ANOVA with Sidak's post-hoc test).
doi:10.1371/journal.pone.0113070.g003

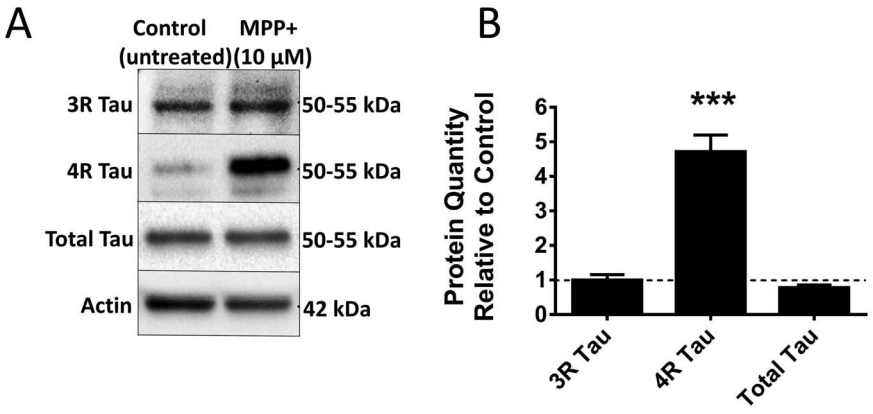

Figure 4. The 4R Isoform was upregulated in the protein level with MPP^+ treatment. A) 4R isoform protein is upregulated with MPP^+ treatment. Western blot for 3R and 4R isoforms of tau protein, as well as total tau (detected with the HT7 antibody). LUHMES cells were either left untreated or treated with 10 µM MPP^+. Actin was used as loading control. B) Quantification of figure 1G. Results show the relative quantity compared to the untreated control cells (dotted line). 3 biological repeats. ***: $p<0.001$ vs. untreated cells (2-way ANOVA with Sidak's post-hoc test).
doi:10.1371/journal.pone.0113070.g004

Discussion

Mitochondrial Complex I Inhibition Reproduces the 4R Isoform Shift Seen in Several Tauopathies

In this paper we have been able to add the increase in 4R tau isoforms as an additional feature to the list of characteristics of PSP that annonacin treatment reproduces in cell culture. This makes annonacin treated neurons a good model for PSP and potentially other sporadic 4R tauopathies. It is unique in the fact that it does not rely on any genetic modification of the *MAPT* gene or artificial overexpression. The fact that it reliably produces an increase in the 4R tau isoforms would also allow it to be used to screen, test and develop candidate drugs targeting tau alternative splicing – something that would not be possible with overexpression-based models of tauopathy.

However, the effect on alternative splicing is not specific to annonacin. Rather, it seems to be related to mitochondrial complex I inhibition more generally. This is suggested by the fact that we have observed the same increase in 4R tau isoforms with MPP^+, another complex I inhibitor. In fact, other features of tauopathy have also been reproduced by other complex I inhibitors [24,25]. However, due to the epidemiological evidence from Guadeloupe strongly linking annonacin consumption to a PSP-like tauopathy, annonacin makes a particularly convincing case as a cell culture based model for PSP. The only drawback of this model relying on immature human neurons is that despite the upregulation of 4R tau, after 10 days there still appears to be overall more 3R than 4R tau, whereas in adult human brain neurons, 3R and 4R are more or less balanced.

However, it is not yet fully understood to what extent the relative increase in the 4R tau isoform contributes to neurotoxicity or impairment of neural functioning. 4R tau isoform increases are only seen in a selection of tauopathies and are region specific. In Alzheimer's disease, there is no abnormal upregulation of 4R isoforms. In PSP, there is some evidence that the 4R isoform may not be upregulated in the frontal cortex, despite the existence of tau pathology in this region [26]. On the other hand, patients with FTDP-17 due to mutations that exclusively affect tau alternative splicing and result in an increase of 4R tau, are evidence that an upregulation of the 4R isoforms is sufficient to start tau aggregation [2,6].

SRSF2 Forms the Link Between Complex I Inhibitors and the Increase in 4R Isoforms

We have identified SRSF2 as a mediator essential for mitochondrial complex I inhibitor induced exon 10 inclusion. The fact that a knockdown of SRSF2 reverses the annonacin induced increase in 4R tau confirms that SRSF2 plays a necessary role for this isoform shift.

SRSF2 is controlled by several kinases including SRPK, AKT, topoisomerase I and CLK/STY family kinases, as well as lysine acetylation [27]. The histone deacetylase inhibitor sodium butyrate has already been demonstrated to increase SRSF2 levels [28], whilst the kinase activity of topoisomerase I can be inhibited with the antitumour drug NB-506 [9]. This suggests that, at least indirectly, SRSF2 is a potentially drugable target.

In our annonacin-treated cell cultures, which might be considered to be an acute model of a sporadic tauopathy, inhibition of SRS2 prevented the 4R isoform shift of tau but not the cell death induced by annonacin. This suggests that, in this model, the 4R tau is not necessary for cell death, since neurons might rather die from reduced energy production [18]. This does, however, not exclude that in a more chronic situation with even higher levels of 4R tau this isoform shift may become the predominant cause of neuronal dysfunction and death.

Complex I Inhibition Is Unlikely to Explain All of the Increase in 4R Isoforms in PSP

In human PSP patients both the SRSF2 and TRA2B splicing factors are upregulated. This suggests that the 4R upregulation is not exclusively due to complex I inhibition, as in that case we would have expected only SRSF2 to be upregulated. Therefore, exploring upstream events leading to TRA2B upregulation may lead to insights on further reasons for the increase in 4R tau isoforms in some tauopathies. It would also be interesting to compare the splicing factor expression levels in 3R tauopathies versus 4R tauopathies.

If SRSF2 is confirmed to be a key player in mediating the 4R isoform upregulation in PSP and other 4R tauopathies, this would make it a suitable drug target for reducing this isoform shift.

Conclusion

In summary, we can conclude that SRSF2 is a necessary mediator for mitochondrial complex I inhibitor induced tau 4R isoform upregulation. As SRSF2 is also increased in PSP patients this suggests mitochondrial complex I inhibition may play at least a partial role in the pathogenesis of 4R tauopathies such as PSP. However, other mechanisms are also likely to contribute.

Acknowledgments

Mr Robin Konhäuser and Ms Magda Baba were instrumental in maintaining the cell lines and cell culture. We would like to acknowledge the Netherlands Brain Bank for their generous contribution of the human brain tissue samples.

Author Contributions

Conceived and designed the experiments: JB HX GUH. Performed the experiments: JB HX. Analyzed the data: JB HX ADA. Contributed reagents/materials/analysis tools: ADA. Wrote the paper: JB HX GUH.

References

1. Williams DR (2006) Tauopathies: classification and clinical update on neurodegenerative diseases associated with microtubule-associated protein tau. Intern Med J 36: 652–660.
2. Liu F, Gong CX (2008) Tau exon 10 alternative splicing and tauopathies. Mol Neurodegener 3: 8.
3. Chen S, Townsend K, Goldberg TE, Davies P, Conejero-Goldberg C (2010) MAPT isoforms: differential transcriptional profiles related to 3R and 4R splice variants. J Alzheimers Dis 22: 1313–1329.
4. Buee L, Delacourte A (1999) Comparative biochemistry of tau in progressive supranuclear palsy, corticobasal degeneration, FTDP-17 and Pick's disease. Brain Pathol 9: 681–693.
5. Zhou J, Yu Q, Zou T (2008) Alternative splicing of exon 10 in the tau gene as a target for treatment of tauopathies. BMC Neurosci 9 Suppl 2: S10.
6. Spillantini MG, Murrell JR, Goedert M, Farlow MR, Klug A, et al. (1998) Mutation in the tau gene in familial multiple system tauopathy with presenile dementia. Proc Natl Acad Sci U S A 95: 7737–7741.
7. Avale ME, Rodriguez-Martin T, Gallo JM (2013) Trans-splicing correction of tau isoform imbalance in a mouse model of tau mis-splicing. Hum Mol Genet 22: 2603–2611.
8. Will CL, Luhrmann R (2011) Spliceosome structure and function. Cold Spring Harb Perspect Biol 3.
9. Pilch B, Allemand E, Facompre M, Bailly C, Riou JF, et al. (2001) Specific inhibition of serine- and arginine-rich splicing factors phosphorylation, spliceosome assembly, and splicing by the antitumor drug NB-506. Cancer Res 61: 6876–6884.

10. Zhong XY, Ding JH, Adams JA, Ghosh G, Fu XD (2009) Regulation of SR protein phosphorylation and alternative splicing by modulating kinetic interactions of SRPK1 with molecular chaperones. Genes Dev 23: 482–495.
11. Swerdlow RH, Golbe LI, Parks JK, Cassarino DS, Binder DR, et al. (2000) Mitochondrial dysfunction in cybrid lines expressing mitochondrial genes from patients with progressive supranuclear palsy. J Neurochem 75: 1681–1684.
12. Lenaz G, Baracca A, Fato R, Genova ML, Solaini G (2006) Mitochondrial Complex I: structure, function, and implications in neurodegeneration. Ital J Biochem 55: 232–253.
13. Stamelou M, de Silva R, Arias-Carrion O, Boura E, Hollerhage M, et al. (2010) Rational therapeutic approaches to progressive supranuclear palsy. Brain 133: 1578–1590.
14. Albers DS, Swerdlow RH, Manfredi G, Gajewski C, Yang L, et al. (2001) Further evidence for mitochondrial dysfunction in progressive supranuclear palsy. Exp Neurol 168: 196–198.
15. Stamelou M, Pilatus U, Reuss A, Magerkurth J, Eggert KM, et al. (2009) In vivo evidence for cerebral depletion in high-energy phosphates in progressive supranuclear palsy. J Cereb Blood Flow Metab 29: 861–870.
16. Lannuzel A, Michel PP, Hoglinger GU, Champy P, Jousset A, et al. (2003) The mitochondrial complex I inhibitor annonacin is toxic to mesencephalic dopaminergic neurons by impairment of energy metabolism. Neuroscience 121: 287–296.
17. Lannuzel A, Hoglinger GU, Verhaeghe S, Gire L, Belson S, et al. (2007) Atypical parkinsonism in Guadeloupe: a common risk factor for two closely related phenotypes? Brain 130: 816–827.
18. Escobar-Khondiker M, Hollerhage M, Muriel MP, Champy P, Bach A, et al. (2007) Annonacin, a natural mitochondrial complex I inhibitor, causes tau pathology in cultured neurons. J Neurosci 27: 7827–7837.
19. Yamada ES, Respondek G, Mussner S, de Andrade A, Hollerhage M, et al. (2014) Annonacin, a natural lipophilic mitochondrial complex I inhibitor, increases phosphorylation of tau in the brain of FTDP-17 transgenic mice. Exp Neurol 253C: 113–125.
20. Lotharius J, Falsig J, van Beek J, Payne S, Dringen R, et al. (2005) Progressive degeneration of human mesencephalic neuron-derived cells triggered by dopamine-dependent oxidative stress is dependent on the mixed-lineage kinase pathway. J Neurosci 25: 6329–6342.
21. Scholz D, Poltl D, Genewsky A, Weng M, Waldmann T, et al. (2011) Rapid, complete and large-scale generation of post-mitotic neurons from the human LUHMES cell line. J Neurochem 119: 957–971.
22. Silver IA, Erecinska M (1994) Extracellular glucose concentration in mammalian brain: continuous monitoring of changes during increased neuronal activity and upon limitation in oxygen supply in normo-, hypo-, and hyperglycemic animals. J Neurosci 14: 5068–5076.
23. Glinka Y, Gassen M, Youdim MB (1997) Mechanism of 6-hydroxydopamine neurotoxicity. J Neural Transm Suppl 50: 55–66.
24. Schapira AH (2010) Complex I: inhibitors, inhibition and neurodegeneration. Exp Neurol 224: 331–335.
25. Hoglinger GU, Lannuzel A, Khondiker ME, Michel PP, Duyckaerts C, et al. (2005) The mitochondrial complex I inhibitor rotenone triggers a cerebral tauopathy. J Neurochem 95: 930–939.
26. Chambers CB, Lee JM, Troncoso JC, Reich S, Muma NA (1999) Overexpression of four-repeat tau mRNA isoforms in progressive supranuclear palsy but not in Alzheimer's disease. Ann Neurol 46: 325–332.
27. Edmond V, Moysan E, Khochbin S, Matthias P, Brambilla C, et al. (2011) Acetylation and phosphorylation of SRSF2 control cell fate decision in response to cisplatin. EMBO J 30: 510–523.
28. Edmond V, Brambilla C, Brambilla E, Gazzeri S, Eymin B (2011) SRSF2 is required for sodium butyrate-mediated p21(WAF1) induction and premature senescence in human lung carcinoma cell lines. Cell Cycle 10: 1968–1977.

J Neuropathol Exp Neurol
Vol. 74, No. 8
August 2015
pp. 850–857

ORIGINAL ARTICLE

Early Neurodegeneration in the Brain of a Child Without Functional PKR-like Endoplasmic Reticulum Kinase

Julius Bruch, MBBChir, Carolin Kurz, MD, Alexandre Vasiljevic, MD, Marc Nicolino, MD, Thomas Arzberger, MD, and Günter U. Höglinger, MDF

Abstract

We report the first detailed examination of the brain of a patient with Wolcott-Rallison syndrome. Wolcott-Rallison syndrome is an extremely rare clinical manifestation of a lack of protein kinase R–like endoplasmic reticulum kinase (PERK) function caused by mutations in the PERK gene *EIF2AK3*. Protein kinase R–like endoplasmic reticulum kinase is thought to play a significant pathogenetic role in several neurodegenerative diseases, including Alzheimer disease, other tauopathies, and Parkinson disease. The brain of a male patient aged 4 years 7 months showed pathologic and immunohistochemical evidence that the absence of PERK for several years is sufficient to induce early changes reminiscent of various neurodegenerative conditions. These include neurofibrillary tangles (as in progressive supranuclear palsy), FUS-immunopositive and p62-immunopositive neurons, and reactive glial changes. We also detected an increased amount of p62-positive puncta coimmunostaining for LC3 and ubiquitin, suggesting changes in autophagic flux. Studying a human brain with absent PERK function presents the opportunity to assess the long-term consequences of nonfunctioning of PERK in the presence of all of the compensatory mechanisms that are normally active in a living human, thereby confirming the importance of PERK for autophagy in the brain and for neurodegeneration.

Key Words: Alzheimer disease, Autophagy, FUS, p62, Parkinson disease, PERK, Tau, Wolcott-Rallison syndrome.

INTRODUCTION

Wolcott-Rallison syndrome (WRS) is the clinical manifestation of a lack of function of protein kinase R–like endoplasmic reticulum kinase (PERK). The syndrome was first described by Wolcott and Rallison (1) in 1972 in a series of 3 siblings. To date, approximately 60 cases have been described in the literature. They largely occur in geographic areas with high levels of consanguinity, such as the Middle East, north Africa, Pakistan, and Turkey. Wolcott-Rallison syndrome is an autosomal recessive condition with manifestations of infancy-onset diabetes mellitus, multiple epiphyseal dysplasia, osteopenia, microcephaly, mental retardation or developmental delay, and hepatic and renal dysfunction (2).

Histologic studies of the bone, pancreas, and liver—but not the brain—of patients with WRS have been performed. Bone tissue shows an irregular proliferation of chondrocytes, spongy bone, and ramified collagen fibers (3). Liver tissue outside phases of hepatic failure shows progressive fibrosis with mild steatosis and noninflammatory necrosis (2, 4). Pancreatic tissue shows severe reduction in acinar tissue and severe β cell deficit with evidence of necrosis (2). Similar findings have also been found in PERK$^{-/-}$ mice (5). Examination of neural function in mice with brain-specific deletion of PERK also shows impaired behavioral flexibility (6).

Wolcott-Rallison syndrome is generally caused by mutations in the *EIF2AK3* gene, which encodes PERK (7); however, mutations in other genes related to PERK function, such as *IER3IP*, have also been implicated (8). Protein kinase R–like endoplasmic reticulum kinase is part of the unfolded protein response, which coordinates cellular responses to an accumulation of unfolded or misfolded proteins in the endoplasmic reticulum. Protein kinase R–like endoplasmic reticulum kinase phosphorylates 2 known downstream targets: EIF2A and NRF2 (9). Phosphorylated EIF2A reduces the rate of translation of most proteins and selectively enhances ATF4 translation, which in turn promotes autophagy (10, 11) and affects mitochondrial protection (12). NRF2, meanwhile, acts to protect cells from oxidative stress (9, 13).

Protein kinase R–like endoplasmic reticulum kinase activity has recently attracted attention in the field of neurodegeneration (14–16). Phosphorylated (i.e. activated) PERK has been detected in the brains of patients with Alzheimer disease (17), Parkinson disease (18), and progressive supranuclear palsy (19), among others. A genomewide association study of progressive supranuclear palsy showed that *EIF2AK3* is genetically associated with the disease (20). One of the mechanisms by which PERK is thought to play a role in neurodegeneration is through its function in regulating autophagy

From the Department of Translational Neurodegeneration, German Center for Neurodegenerative Diseases (DZNE) Munich (JB, CK, GUH); Department of Neurology, Technische Universität München (JB, CK, GUH); Department of Psychiatry and Psychotherapy (TA) and Center for Neuropathology and Prion Research (TA), Ludwig Maximilians Universität, Munich, Germany; and Department of Pathology and Neuropathology, Groupement Hospitalier Est, Bron (AV), and Division of Pediatric Endocrinology, Lyon University Pediatric Hospital, Lyon (MN), France.

Send correspondence and reprint requests to: Günter U. Höglinger, MD, Department of Translational Neurodegeneration, German Center for Neurodegenerative Diseases, Feodor-Lynen Str. 17, Munich 81377, Germany; E-mail: guenter.hoeglinger@dzne.de

Julius Bruch was funded by the Bavarian Research Foundation (Bayerische Forschungsstiftung). Günter U. Höglinger was funded by DFG (Deutsche Forschungsgemeinschaft; Grant No. HO2402/6-2).

The authors declare no conflicts of interest.

TABLE 1. Human Tissue Samples

Case No.	Diagnosis	Cause of Death	Age at Death (years)	Sex	Postmortem Delay
WRS	WRS	Hepatic and renal failure	4	Male	Unknown
C1	Control	Pulmonary hypertension	3	Male	48 hours
C2	Control	Aplastic anemia	6.5	Male	24 hours
C3	Control	Pneumonia	4	Male	65 hours

(10, 11, 21) and other cell protective mechanisms, such as oxidative stress defense (9). Autophagy is thought to be critical to the health of neurons because they cannot rely on mitosis to rid themselves of excess proteins and cellular material (22). In fact, stimulation of autophagy has been shown to mitigate pathology in models of Alzheimer disease, other tauopathies, and Parkinson disease (22–25).

The present study presents the first immunohistochemical examination of the brain of a patient with WRS. In light of recent developments in the role of PERK in neurodegeneration, we examined the brain of a 4-year-old boy with WRS for findings of neurodegenerative diseases.

MATERIALS AND METHODS

Search for Tissue From Patients With WRS

We started our search for WRS postmortem brain material by contacting all institutions that had published cases of the syndrome or had written about the syndrome in PubMed-listed literature. This step yielded samples of 1 patient from Lyon University Pediatric Hospital (Lyon, France) in which *EIF2AK3* had previously been identified as the gene responsible for WRS. Next, we searched the Brain Net Europe database and contacted leading pediatric units across the world. We were unable to find brain material from additional WRS cases with confirmed *EIF2AK3* mutations.

Genotyping

DNA was extracted from peripheral blood collected on EDTA. The diagnosis of WRS was confirmed by direct sequencing of *EIF2AK3* on genomic DNA, as previously described (5). This showed a c.3009C→T substitution that is homozygous in the patient and heterozygous in the parents, resulting in a p.R903* nonsense mutation and a truncated protein.

Postmortem Tissue

Three blocks (2 blocks from the frontal cortex and 1 block from the cerebellum) of paraffin-embedded tissue from a single patient were obtained from the Department of Pathology and Neuropathology, Groupement Hospitalier Est (Bron, France). The parents had given full permission for the use of the material and medical records for research purposes, according to the Declaration of Helsinki. Equivalent blocks of paraffin-embedded tissue from 3 age-matched control cases were obtained from the Center for Neuropathology and Prion Research, University of Munich (Munich, Germany). These were anonymized routine biopsy cases. The use of the material was in accordance with the directives of the local ethics commission regarding the use of archive material for research purposes. Table 1 shows an overview of the cases described.

Immunohistochemistry

The paraffin blocks were cut on a microtome to a thickness of 5 μm. Tissue was deparaffinized and progressively rehydrated according to the Abcam protocol (www.abcam.com/protocols). Hematoxylin and eosin (Hoffmann-LaRoche, Basel, Switzerland) staining was performed according to the manufacturer's guidelines. Antigen retrieval was performed by heating slides in 10 mmol/L sodium citrate (Sigma-Aldrich, St Louis, MO) buffer at 90°C for 20 minutes. Immunohistochemical staining was performed semiautomatically on a BenchMark IHC device (Ventana, Tucson, AZ [now Hoffmann-LaRoche]). The primary antibodies, concentrations, and incubation times used are shown in Table 2. iView DAB and ultraView DAB (Perkin-Elmer, Waltham, MA) were used as detection systems. Nuclear counterstaining was performed with hematoxylin (Hoffmann-LaRoche). Microscopy and imaging were performed on a Leica CTR 6000 microscope (Leica Microsystems, Wetzlar, Germany).

Double-Label Immunofluorescence

Tissue sections were cut, deparaffinized, and rehydrated, and antigens were retrieved, as described previously. The slides were blocked in 5% normal goat serum (Vector Laboratories, Burlingame, CA) in phosphate-buffered saline (PBS) with 0.2% Tween (Sigma-Aldrich). Primary antibody was incubated in 2% normal goat serum in PBS with 0.2% Tween overnight at 4°C. The antibodies and concentrations used are listed in Table 2. The slides were washed 3 times for 5 minutes in PBS and incubated for 2 hours in 2% normal goat serum in PBS with 0.2% Tween at room temperature with the fluorescent secondary antibodies Alexa Fluor 488 goat anti-mouse IgG (Life Technologies [now Thermo-Fisher Scientific, Carlsbad, CA]) and Alexa Fluor 594 goat anti-rabbit IgG (Life Technologies). DAPI dihydrochloride (Thermo-Fisher Scientific) 300 nmol/L was added and incubated for 10 minutes. The slides were washed 3 times for 5 minutes in PBS and coverslipped with polyvinyl alcohol mounting medium with DABCO antifading mounting medium (Sigma-Aldrich). Microscopy and imaging were performed on a Leica TCS SP5 II laser confocal microscope (Leica Microsystems).

RESULTS

Clinical Case History

The patient (Case 2 in [26]) was a 4-year-old boy born to consanguineous Kosovar parents. He showed the first signs of diabetes mellitus at age 6 months, which were treated with

TABLE 2. Primary Antibodies and Immunostaining Conditions

Antigen	Clone	Species	Incubation Time	Temperature	Concentration	Detection System	Source
PHF tau	AT8	Mouse	1 hour	RT	1:200	iView DAB (Perkin-Elmer)	Thermo-Fisher Scientific (Rockford, IL)
Glial fibrillary acidic protein	GA5	Mouse	1 hour	RT	1:100	iView DAB (Perkin-Elmer)	Cell Signaling Technology (Beverly, MA)
p62 Lck ligand	3	Mouse	1 hour	RT	1:100	iView DAB (Perkin-Elmer)	BD Biosciences (Franklin Lakes, NJ)
Ubiquitin	Polyclonal	Rabbit	Overnight	4°C	1:100	Fluorescence	Abcam (Cambridge, United Kingdom)
Cleaved caspase 3	D3E9	Rabbit	Overnight	4°C	1:100	iView DAB (Perkin-Elmer)	Cell Signalling
NeuN	Polyclonal	Rabbit	Overnight	4°C	1:200	iView DAB (Perkin-Elmer)	EMD Millipore (Billerica, MA)
α-Synuclein	42	Mouse	1 hour	RT	1:2000	ultraView DAB (Perkin-Elmer)	BD Biosciences
LC3B	D11	Rabbit	Overnight	4°C	1:100	Fluorescence	Cell Signaling
FUS	Polyclonal	Rabbit	1 hour	RT	1:100	ultraView DAB (Perkin-Elmer)	Bethyl Laboratories (Montgomery, TX)
pTDP-43	Polyclonal	Rat	1 hour	RT	1:50	ultraView DAB (Perkin-Elmer)	Own production by cooperation partner
β-Amyloid	6E10	Mouse	1 hour	RT	1:2000	iView DAB (Perkin-Elmer)	Covance (Princeton, NJ)
Microglial NP_001614 and NP_116573	Iba1	Rabbit	1 hour	RT	1:500	iView DAB (Perkin-Elmer), microwave pretreatment	Wako (Richmond, VA)
Activated microglia	CR3/43	Mouse	1 hour	RT	1:100	iView DAB (Perkin-Elmer)	Dako (Glostrup, Denmark)

PHF, paired helical filament; RT, room temperature.

twice daily insulin injections. A clinical diagnosis of WRS was made only at age 4 years when he first presented to the Lyon University Pediatric Hospital together with his older sister, who was also affected.

At the time of diagnosis, the glycated hemoglobin level was 8.6%. Radiographs showed skeletal dysplasia in carpal bones and phalanges, capital femoral epiphyses, and vertebral bodies. There were no further abnormalities on ultrasound examination of organs or on liver and kidney function tests. No neurologic abnormality was noted.

Six months later, at age 4 years 7 months, the patient presented to the intensive care unit of the Lyon University Pediatric Hospital with sudden-onset coma, vomiting, hepatomegaly (7 cm), tachycardia (111 beats/minute), and mild pyrexia. Blood pressure dropped from 90/46 mm Hg initially to 53/27 mm Hg. There was coagulopathy (factor V, 14%; prothrombin time, 13 seconds; fibrinogen, 0.9 g/L). Liver function values were outside the reference range (ammonia, 859 μmol/L; lactate, 17.6 mmol/L; alanine aminotransferase, 8,000 IU/L; aspartate aminotransferase, 16,000 IU/L). Renal function was also compromised, with a potassium level of 6.6 mEq/L and a serum creatinine level of 270 μmol/L. Diagnoses of hepatic encephalopathy and renal failure were made. Treatment was supportive (with mechanical ventilation) until death occurred by vascular hypotension and ventricular arrhythmia.

Genetics

Genetic testing revealed the patient to be homozygous for the mutation *R902stop* in the *EIF2AK3* gene. This mutation has been described before in 2 siblings of Kosovo-Albanian origin with similar clinical history (27). The mutation leads to truncation of the PERK protein, eliminating almost the entire second active site of PERK (Fig. 1). This suggests that PERK in this patient is present as a truncated, functionally inactive fragment.

General Autopsy Findings

No external abnormity, except for delayed growth and reduced body weight (12 kg), was noted. The liver was enlarged (722 g), showing mildly expanded and inflamed portal

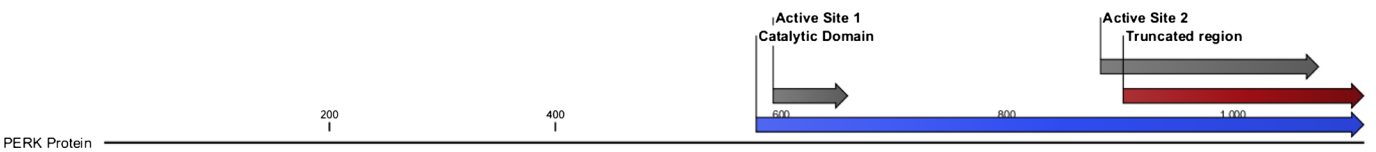

FIGURE 1. Functional PERK protein primary structure and *R902stop* mutation. The PERK protein has an endoplasmic reticulum luminal domain and a cytoplasmic catalytic domain (blue arrow); the latter contains 2 active sites (gray arrows). The mutation *R902stop* results in truncation of much of the second active site (red arrow). This figure was created using CLC Main Workbench 6.9 (Qiagen, Venlo, The Netherlands).

tracts and hypereosinophilic or vacuolated hepatocytes. The pancreas was small (20 g) with hypereosinophilic exocrine tissue. Results of the full pathologic examination are described in the study by Collardeau-Frachon et al (26).

Because the brain was not the center of attention at the time of autopsy examination, only limited information was recorded. There was slight cerebral edema with early tonsillar herniation. Gyration was not abnormal, but sections had pale appearance. No vascular abnormality or focal lesion was observed. The cerebellum and brainstem had no macroscopic abnormality. No brain weight or size was recorded.

Histologic Findings

Hematoxylin and eosin staining of the frontal cortex and cerebellum showed reduced cell density in the molecular layer, compared with age-matched control cases (Fig. 2). The subpial region of the molecular layer was irregularly rarefied. No overt oligodendrocyte pathology was noted, and there was no evidence of proteinaceous inclusions in oligodendrocytes, such as coiled bodies. Luxol fast blue–periodic acid Schiff myelin staining did not show any abnormality of white matter tracts. On NeuN immunostaining, there was no visible abnormality of layering.

Immunostaining for glial fibrillary acidic protein revealed unusually prominent and corkscrew-like extensions of Bergmann glial cells in the cerebellum (Fig. 3B) that were not present in normal controls (Fig. 3A). Glial fibrillary acidic protein staining also showed focal clusters of activated astrocytes, especially in the subpial region of the cortex (Fig. 3D), which were much larger than those in control cases (Fig. 3C). These findings are consistent with long-term gliosis. To investigate this further, we stained for microglia with the Iba1 marker (Figs. 3E, F). The WRS brain showed higher density and some clustering of microglia compared with the 3 control brains. Staining for the activated microglia marker CR3/43 in the WRS brain, however, yielded negative results.

There were individual neurons with FUS-positive inclusions (Figs. 4A, B), which are associated with certain types of frontotemporal dementia (28). Other neurons stained positive for AT8 (Figs. 4C, D), an antibody against phosphorylated paired helical filament tau; AT8-positive tau is considered to be pathologic (29). The appearance was that of a globose neurofibrillary tangle, possibly suggesting the beginnings of tau pathology akin to that in progressive supranuclear palsy. These findings were absent in the 3 control cases and in cerebellar tissue.

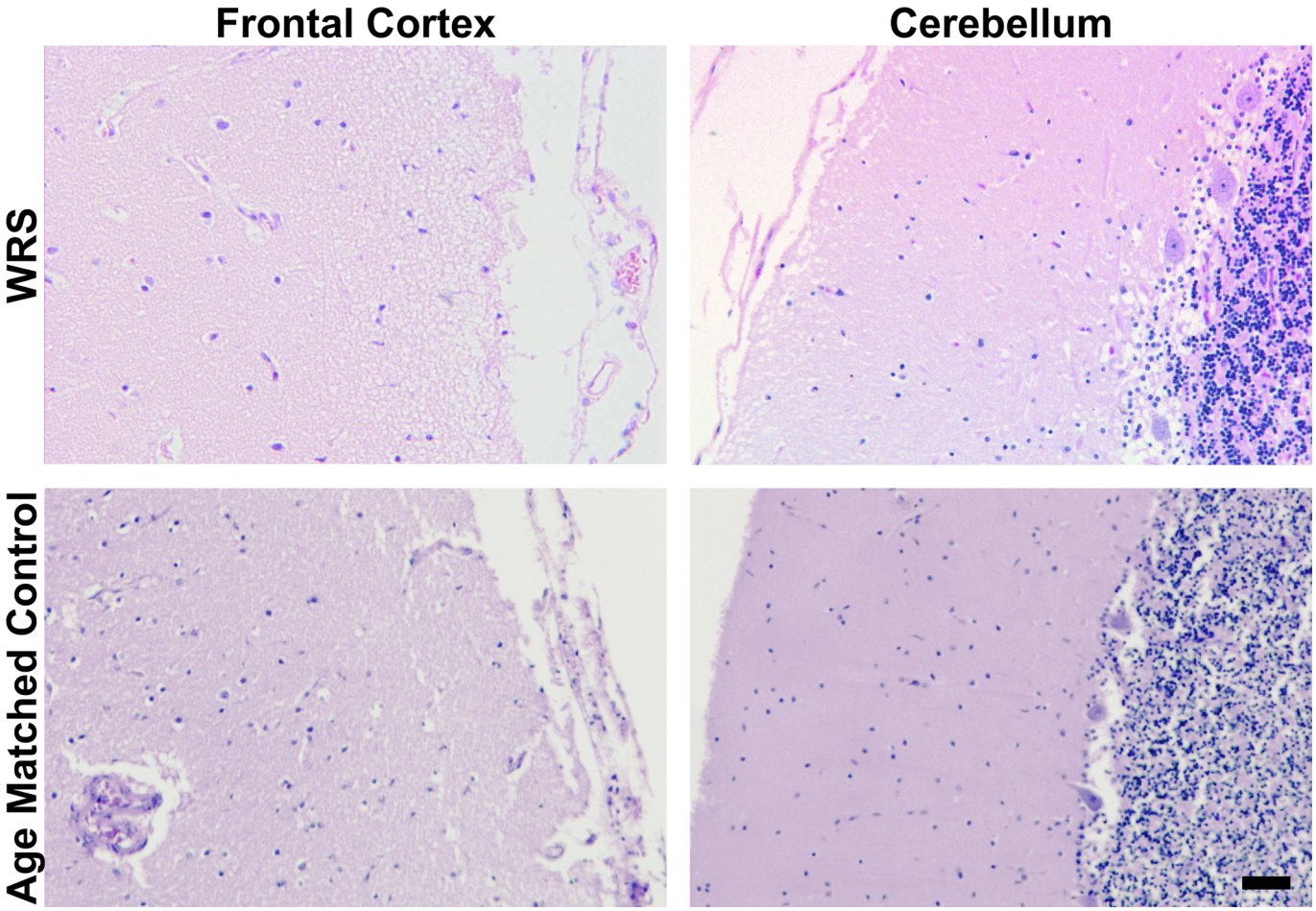

FIGURE 2. Hematoxylin and eosin staining (10×) of sections of the frontal cortex and cerebellum. There was reduced cell density in the molecular layer of the cerebellum and in the outer gray matter layers of the frontal cortex in the WRS case compared with age-matched controls. Scale bar = 50 μm.

The WRS brain yielded negative immunostaining for α-synuclein, β-amyloid, and TDP-43 aggregates and for cleaved caspase 3 (positive control: lymphoma). Gallyas staining also did not reveal any abnormal changes (data not shown).

Impairment of Autophagic Flux

We looked further into the impact of absent PERK function in this brain on autophagy. We saw several cells that were positive for p62, a marker that can accumulate in cells with interrupted autophagic flux (Figs. 4E, F). These were not observed in the age-matched control brains.

Using double-label immunofluorescent laser confocal microscopy, we observed p62 in scattered puncta in a wide distribution in the WRS brain; some cells had pronounced density (Fig. 5A). Although there were fewer puncta that were positive for p62 than for LC3 overall, there was considerable overlap. As expected, there was also a high level of overlap of p62 with ubiquitin (Fig. 5B). The control brains showed virtually no such p62-positive puncta.

DISCUSSION

Examination of samples from the brain of a 4-year-old boy without PERK function presented a unique opportunity to

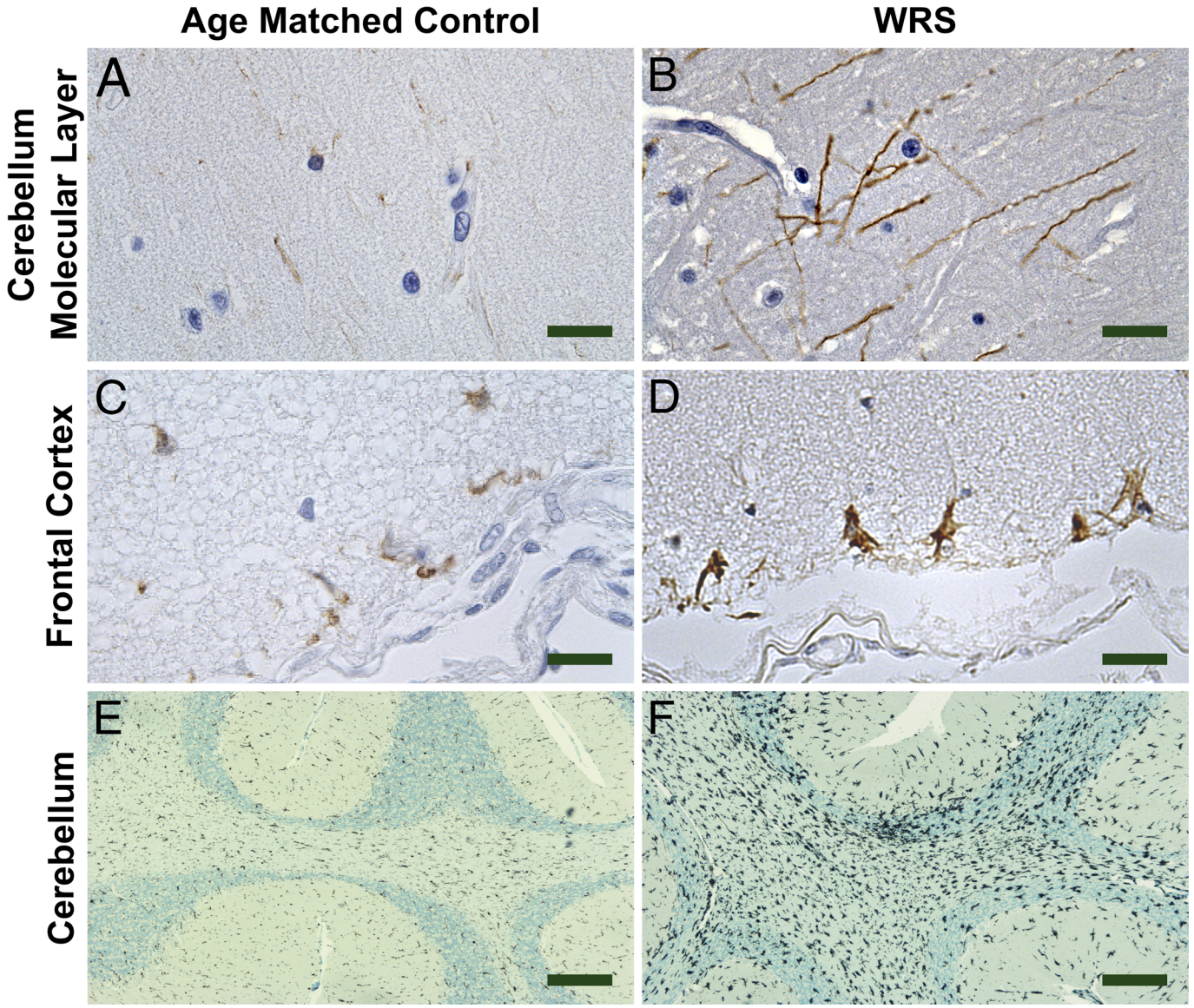

FIGURE 3. Glial histology. **(A)** Glial fibrillary acidic protein immunostaining (63×) with hematoxylin counterstaining in a control brain shows only thin straight processes of Bergmann glial cells. **(B)** Glial fibrillary acidic protein immunostaining (63×) with hematoxylin counterstaining in the WRS brain shows thickened and corkscrew-like processes of Bergmann glial cells. **(C)** Glial fibrillary acidic protein immunostaining (63×) in a control brain shows a normal pattern of glial fibrillary acidic protein–positive astrocytes. **(D)** Glial fibrillary acidic protein immunostaining (63×) in the WRS brain shows a cluster of reactive enlarged astrocytes adjacent to the pia mater. **(E)** Iba1 immunostaining (4×) of the cerebellum of a control brain showing normal distribution of microglia. Scale bar = 350 μm. **(F)** Iba1 immunostaining (4×) of the cerebellum of the WRS case shows increased density and clustering of microglia. Scale bars = **(A–D)** 20 μm; **(E, F)** 350 μm.

learn about the effects of PERK dysfunction without the limitations of animal models and short-term cell culture models.

We found evidence that a lack of PERK function for several years is sufficient to induce changes reminiscent of the early stages of several neurodegenerative diseases (i.e. formation of globose AT8-positive neurofibrillary tangles typical of tauopathies and FUS-positive neurons occurring in some forms of frontotemporal dementia). There were generally only small numbers of cells affected by these immunohistochemical changes; however, these findings were completely absent

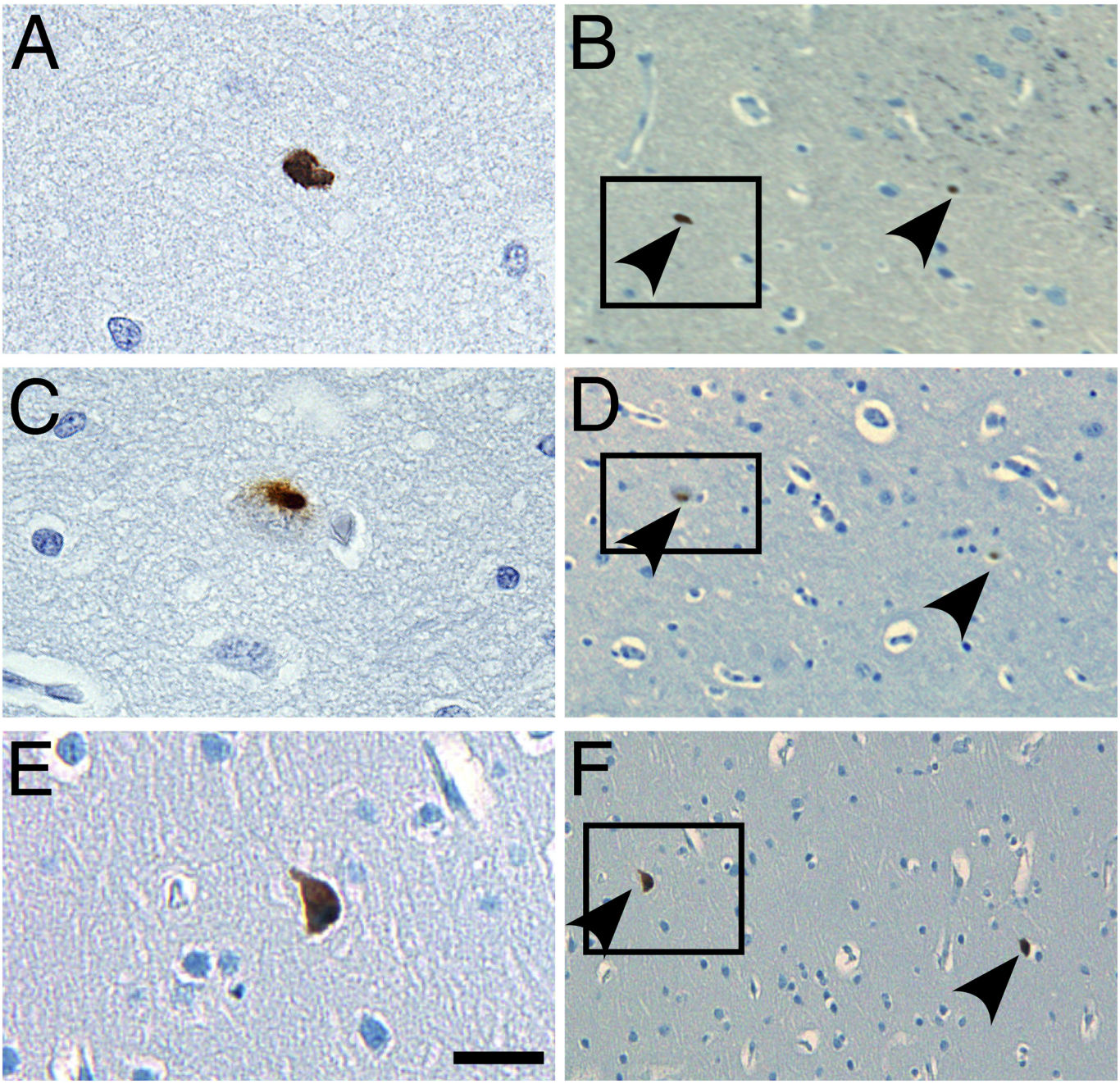

FIGURE 4. Immunohistochemical findings for the frontal cortex of the WRS brain. **(A)** FUS immunostaining shows an individual FUS-positive neuron. Original magnification: 63×. **(B)** FUS immunostaining shows 2 immunopositive neurons. The box indicates the field shown in **(A)**. Original magnification: 10×. FUS-positive cells were generally farther apart. **(C)** AT8 tau immunostaining showing globose neurofibrillary tangles in the cytoplasm of a neuron. Original magnification: 63×. **(D)** AT8 tau immunostaining showing 2 immunopositive neurons, including the one shown in the box in **(C)**. Original magnification: 10×. Positive cells were generally farther apart. **(E)** p62 immunostaining showing an immunopositive cell. Original magnification: 63×. **(F)** p62 immunostaining showing 2 p62-positive cells. Original magnification: 10×. Immunopositive cells were generally farther apart. Box indicates the field shown in **(E)**. Scale bars = (left column) 10 μm; (right column) 50 μm. Arrowheads point to immunopositive cells.

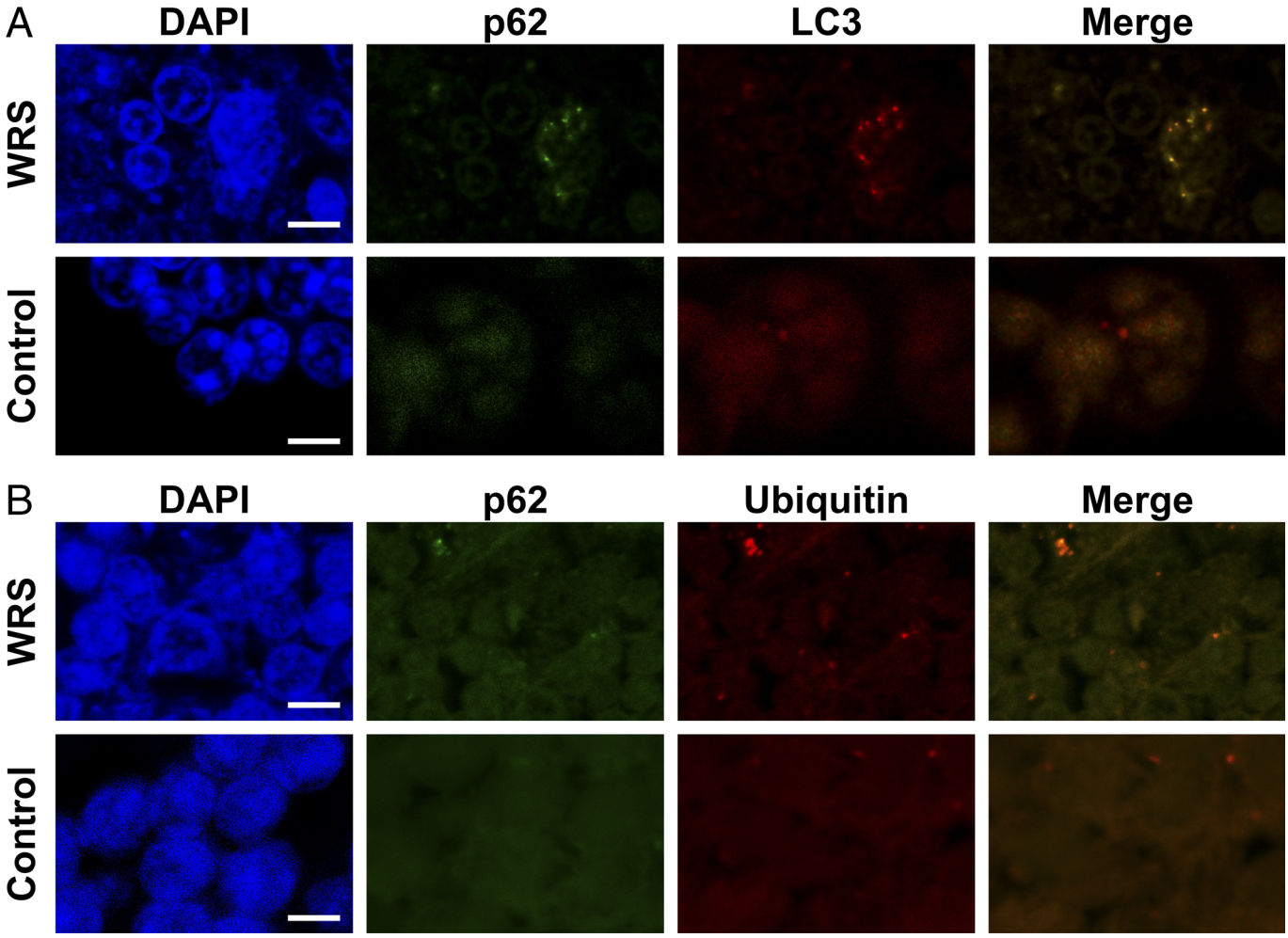

FIGURE 5. p62 colocalization with LC3 and ubiquitin. **(A, B)** Immunofluorescent laser confocal images of the cerebella of the patient with WRS and a representative age-matched control patient. Puncta of p62 staining (green) are evident in some cells in the WRS case but not in the control. These puncta of p62 colocalized with both LC3 (**A**; red), and ubiquitin (**B**; red). There were less LC3 and ubiquitin-positive puncta in the control than in the patient with WRS. DAPI (blue) stains nuclear DNA. Scale bars = 5 μm.

in the 3 age-matched control brains. In addition, there were also changes suggesting activation of astrocytes and Bergmann glial cells, and increased density and clustering of microglia. These may represent process similar to the fibrotic and inflammatory processes observed in other organs of patients with WRS.

We also observed changes suggestive of impaired autophagy. Although there is already an emerging body of knowledge on the role of PERK in regulation of autophagy, the case described allowed, for the first time, an assessment of the impact of absent PERK function for several years on autophagy in a human. In the process of marking misfolded proteins for macroautophagy, proteins get ubiquitinated and tagged with p62, which in turn binds to LC3 proteins on nascent autophagophores. Colocalization of p62, LC3, and ubiquitin in the WRS brain suggests that this process works well in the absence of PERK function. However, the increased amount of p62-positive puncta coimmunostaining for LC3 and ubiquitin and the existence of some cells staining very intensely for p62 suggest that, in numerous cells in the WRS brain, formed vesicles accumulate and do not proceed to lysosomal fusion and degradation. This corresponds to our knowledge that ATF4, the transcription factor acting downstream of PERK, induces a set of autophagy-related genes, including *ATG5*, *ATG7*, and *ATG12*. These genes are involved mainly in the completion and coating of autophagic vesicles. This observation is relevant because autophagy has been implicated in a large number of neurodegenerative conditions.

In conclusion, the present study shows, for the first time, evidence that the absence of PERK is sufficient to induce early changes reminiscent of various human neurodegenerative diseases and confirms the importance of PERK for autophagy in the pathogenesis of neurodegeneration.

ACKNOWLEDGMENTS

Ms Brigitte Kraft performed many of the immunohistochemical stainings. We thank Cécile Julier and Valérie Senée (Inserm UMR-S958, Medical Faculty Paris 7, site Villemin, Paris, France) for their work in mutation analysis. We would like to acknowledge the many people we contacted in our

search for brain autopsy material from WRS cases who searched their databases and brain banks for us.

REFERENCES

1. Wolcott CD, Rallison ML. Infancy-onset diabetes mellitus and multiple epiphyseal dysplasia. J Pediatr 1972;80:292–97
2. Julier C, Nicolino M. Wolcott-Rallison syndrome. Orphanet J Rare Dis 2010;5:29
3. Castelnau P, Le Merrer M, Diatloff-Zito C, Marquis E, Tête MJ, Robert JJ. Wolcott-Rallison syndrome: A case with endocrine and exocrine pancreatic deficiency and pancreatic hypotrophy. Eur J Pediatr 2000;159:631–33
4. Iyer S, Korada M, Rainbow L, et al. Wolcott-Rallison syndrome: A clinical and genetic study of three children, novel mutation in EIF2AK3 and a review of the literature. Acta Paediatr 2004;93:1195–201
5. Harding HP, Zeng H, Zhang Y, et al. Diabetes mellitus and exocrine pancreatic dysfunction in perk$^{-/-}$ mice reveals a role for translational control in secretory cell survival. Mol Cell 2001;7:1153–63
6. Trinh MA, Kaphzan H, Wek RC, Pierre P, Cavener DR, Klann E. Brain-specific disruption of the eIF2alpha kinase PERK decreases ATF4 expression and impairs behavioral flexibility. Cell Rep 2012;1:676–88
7. Delepine M, Nicolino M, Barrett T, Golamaully M, Lathrop GM, Julier C. EIF2AK3, encoding translation initiation factor 2-alpha kinase 3, is mutated in patients with Wolcott-Rallison syndrome. Nat Genet 2000;25:406–9
8. Abdel-Salam GM, Schaffer AE, Zaki MS, et al. A homozygous IER3IP1 mutation causes microcephaly with simplified gyral pattern, epilepsy, and permanent neonatal diabetes syndrome (MEDS). Am J Med Genet A 2012;158A:2788–96
9. Cullinan SB, Zhang D, Hannink M, Arvisais E, Kaufman RJ, Diehl JA. Nrf2 is a direct PERK substrate and effector of PERK-dependent cell survival. Mol Cell Biol 2003;23:7198–209
10. Matsumoto H, Miyazaki S, Matsuyama S, et al. Selection of autophagy or apoptosis in cells exposed to ER-stress depends on ATF4 expression pattern with or without CHOP expression. Biol Open 2013;2:1084–90
11. B'Chir W, Maurin AC, Carraro V, et al. The eIF2alpha/ATF4 pathway is essential for stress-induced autophagy gene expression. Nucleic Acids Res 2013;41:7683–99
12. Bouman L, Schlierf A, Lutz AK, et al. Parkin is transcriptionally regulated by ATF4: Evidence for an interconnection between mitochondrial stress and ER stress. Cell Death Differ 2011;18:769–82
13. Kansanen E, Kuosmanen SM, Leinonen H, Levonen AL. The Keap1-Nrf2 pathway: Mechanisms of activation and dysregulation in cancer. Redox Biol 2013;1:45–49
14. Cornejo VH, Hetz C. The unfolded protein response in Alzheimer's disease. Semin Immunopathol 2013;35:277–92
15. Hetz C, Chevet E, Harding HP. Targeting the unfolded protein response in disease. Nat Rev Drug Discov 2013;12:703–19
16. Hetz C, Mollereau B. Disturbance of endoplasmic reticulum proteostasis in neurodegenerative diseases. Nat Rev Neurosci 2014;15:233–49
17. Hoozemans JJ, van Haastert ES, Nijholt DA, Rozemuller AJ, Eikelenboom P, Scheper W. The unfolded protein response is activated in pretangle neurons in Alzheimer's disease hippocampus. Am J Pathol 2009;174:1241–51
18. Hoozemans JJ, van Haastert ES, Eikelenboom P, de Vos RA, Rozemuller JM, Scheper W. Activation of the unfolded protein response in Parkinson's disease. Biochem Biophys Res Commun 2007;354:707–11
19. Nijholt DA, van Haastert ES, Rozemuller AJ, Scheper W, Hoozemans JJ. The unfolded protein response is associated with early tau pathology in the hippocampus of tauopathies. J Pathol 2012;226:693–702
20. Hoglinger GU, Melhem NM, Dickson DW, et al. Identification of common variants influencing risk of the tauopathy progressive supranuclear palsy. Nat Genet 2011;43:699–705
21. Avivar-Valderas A, Salas E, Bobrovnikova-Marjon E, et al. PERK integrates autophagy and oxidative stress responses to promote survival during extracellular matrix detachment. Mol Cell Biol 2011;31:3616–29
22. Nixon RA. The role of autophagy in neurodegenerative disease. Nat Med 2013;19:983–97
23. Jiang TF, Zhang YJ, Zhou HY, et al. Curcumin ameliorates the neurodegenerative pathology in A53T alpha-synuclein cell model of Parkinson's disease through the downregulation of mTOR/p70S6K signaling and the recovery of macroautophagy. J Neuroimmune Pharmacol 2013;8:356–69
24. Schaeffer V, Lavenir I, Ozcelik S, Tolnay M, Winkler DT, Goedert M. Stimulation of autophagy reduces neurodegeneration in a mouse model of human tauopathy. Brain 2012;135:2169–77
25. Wong E, Cuervo AM. Autophagy gone awry in neurodegenerative diseases. Nat Neurosci 2010;13:805–11
26. Collardeau-Frachon S, Vasiljevic A, Jouvet A, Bouvier R, Senée V, Nicolino M. Microscopic and ultrastructural features in Wolcott-Rallison syndrome, a permanent neonatal diabetes mellitus: About two autopsy cases. Pediatr Diabetes 2014. doi: 10.1111/pedi.12201 [Epub ahead of print]
27. Spehar Uroić A, Mulliqi Kotori V, Rojnić Putarek N, Kušec V, Dumić M. Primary hypothyroidism and nipple hypoplasia in a girl with Wolcott-Rallison syndrome. Eur J Pediatr 2014;173:529–31
28. Snowden JS, Hu Q, Rollinson S, et al. The most common type of FTLD-FUS (aFTLD-U) is associated with a distinct clinical form of frontotemporal dementia but is not related to mutations in the FUS gene. Acta Neuropathol 2011;122:99–110
29. Goedert M, Jakes R, Vanmechelen E. Monoclonal antibody AT8 recognises tau protein phosphorylated at both serine 202 and threonine 205. Neurosci Lett 1995;189:167–69

